

## **GEOCHEMICAL STUDY ON A LIMESTONE/MARLSTONE ALTERNATION, BAJOCIAN, MECSEK MOUNTAINS, SOUTHERN TRANSDANUBIA, HUNGARY**

BÉLA RAUCSIK<sup>1</sup>, GYULA SZABÓ<sup>2</sup>, ILDIKÓ BORBÉLY-KISS<sup>2</sup>

### **ABSTRACT**

A geochemical study of the Bajocian portion of the Komló Calcareous Marl Formation (Mecsek Mountains, southern Hungary) was undertaken in order to characterize the rhythmic alternations of carbonate-rich and carbonate-poor layers and to investigate their possible origin. 45 samples of Komló Calcareous Marl Formation collected from six segments of the outcrops of Püspökszentlászló II. and Kecsegyúr, road cut were examined by PIXE analysis. Concentrations some of the trace elements are higher than can be explained by a pure detrital clastic source. Excess concentrations (over detrital) of these trace elements may be derived from seawater and likely associated with the organic and clay mineral fraction as well as with the carbonate phase.

Limestone semicouplets are characterized by good oxygenation as expressed by the pervasive bioturbation, by the Fe/Mn parameter and by the lack of preserved organic matter. The abundance of silica, phosphorous and strontium in the absence of high terrigenous input suggests that during limestone deposition surface waters were rather highly fertile due to an efficient recycling of nutrients from deeper waters. The enhanced fertility was coupled with a current system at the well-oxygenated seafloor which prevented the accumulation of organic matter and of the organic matter-bound trace elements, such as Zn, Cu and V. During early diagenesis, Mn should migrated from weaker oxic parts of sediment column and precipitated as carbonate and/or as oxide, oxihydroxide coatings on biogenic tests resulting Mn-enrichment in the carbonate-rich semicouplets.

Marly semicouplets deposited under moderately oxic, probably dysoxic conditions (indicated by the high Fe/Mn parameter), which does not allow the preservation of abundant organic matter and the appearance of sedimentary structure as lamination. High TiO<sub>2</sub> and SiO<sub>2</sub> values indicate that marly semicouplets received a substantial contribution from a terrigenous source. Differences in the solubility of reduced iron and manganese could lead to sedimentary fractionation of these elements across redox boundaries resulting Fe-enrichment during deposition of carbonate-poor semicouplets. Trace metals (Zn, Cu, V) were carried as portions of organo-metal complexes and as adsorbed ions on clay minerals in the water column. Disoxic conditions in the sediment mass and at the seafloor were favorable to preservation and accumulation a part of these trace elements. Mainly the V, Zn and Cu abundances in the carbonate-poor layers seem to be accounted by diagenetic enrichment; Ni enrichment is affiliated with the increased terrigenous supply, although some degree of redox-controlled diagenetic modification cannot be excluded. The lower phosphorous abundance in the carbonate-poor semicouplets suggests that the depositional environment should be characterized by lower surface-water fertility and productivity during their deposition.

According to these data and results of formerly stable isotope measurements, the rhythmic organization of couplets should represent climatic changes. Palaeoceanographic conditions alternated from efficiently mixed, highly-fertile surface waters and well-oxygenated seafloor, to enhanced water runoff and/or decreased evaporation with decreased productivity and moderately oxygenated bottom waters. Moderately oxidizing (most likely dysoxic) conditions at the bottom may be caused by water mass stratification. This stratification could have resulted from the presence of a less saline, <sup>18</sup>O-depleted surface-water. The corresponding climatic conditions thus alternated from more arid to more humid.

---

<sup>1</sup> Department of Earth and Environmental Sciences, University of Veszprém, P.O. Box 158, H-8201 Veszprém, Hungary

<sup>2</sup> Institute of Nuclear Research of the Hungarian Academy of Sciences, P.O. Box 51, H-4001 Debrecen, Hungary

## INTRODUCTION

Cyclic sedimentation recorded as lithological rhythmicity (according to the terminology of EINSELE et al., 1991) in pelagic and hemipelagic succession has been the goal of many works in the last years. In many cases, interest has been focused on Cretaceous formations, which are often characterized by cyclicity expressed as alternations of carbonate-rich and carbonate-poor layers. Diagenetic enhancement of the lithological rhythms played an important role in some sequences (RICKEN, 1991, 1994). Jurassic formations has been studied by few workers (MATTIOLI, 1997).

The possible mechanisms that may produce this kind of cyclicity have been attributed to the variation of a single palaeoenvironmental factor or to a combination of several variable factors. These factors include fluctuations in (1) the supply of fine terrigenous sediments (dilution cycles); (2) the supply of calcareous biogenic sediment produced by plankton (productivity cycles); (3) the degree of saturation of seawater with respect to calcium carbonate (dissolution cycles); (4) the availability of oxygen at the sea floor and the degree of organic matter depletion/preservation (redox cycles) (ROCC Group, 1986; FISCHER et al., 1990; DE BOER and SMITH, 1994; SETHI and LEITHOLD, 1994; BELLANCA et al., 1996; BICKERT et al., 1997). Even if Milankovitch-type cyclic patterns might be expressed by a combination of physical, chemical and geological fluctuations, many of the papers emphasized so far the palaeontological aspects in order to explain the mechanisms leading to the deposition of lithological rhythms (BOTTJER et al., 1986; SAVRDA and BOTTJER, 1994; ERBA and PREMOLI SILVA, 1994). A fairly new and less common approach focuses on the geochemical characterization of such couplets. Many recent works have been centered on isotope stratigraphy (WEISSERT and BRÉHÉRET, 1991; Jenkyns et al., 1994; BELLANCA et al., 1996; BICKERT et al., 1997), but much fewer papers used geochemical data in an attempt to understand the palaeoceanographic meaning of the alternations (MURRAY et al., 1990; SUNDARAMAN et al., 1993; BELLANCA et al., 1996). This method has been appearing just sporadically in Hungarian literature (CORNIDES et al., 1979, FOGARASI, 1995). The aim of this paper is to examine the geochemical (major and trace elements) fluctuations occurring within the couplets in the Lower Bajocian interval of Komló Calcareous Marl Formation in order to reconstruct fluctuations in oxygen content at the seafloor and to unravel the climatic significance of the lithologic alternation.

## GEOLOGICAL SETTING

The studied sections are located in the Mecsek Mountains, near the town of Komló (*Fig. 1*). The Mecsek Mountains belongs to the Tisza Terrane, a structural unit of the Pannonian Basin. According to the structure of the outcrops in the Apuseni Mountains (Romania) (BLEAHU 1976; IANOVICI et al. 1976) and to borehole and seismic data from the basement of the Great Hungarian Plain (BALÁZS et al. 1986; FÜLÖP et al. 1987; GROW et al. 1994) the Tisza Terrane is made up of basement nappe systems overthrust with northern vergency during the Cretaceous Austroalpine tectogenesis.

Differentiation of the carbonate shelf - a part of the northern continental margin of the Tethys - into extensional "halfgraben" structures started during the Upper Triassic (NAGY, 1969). This process was continued in the Jurassic in connection with rifting the Penninic Ocean. The Early Liassic in the Mecsek Mountains is characterized by coal and arkose-bearing continental and shallow marine siliciclastic sequence (Gresten facies). In the

Sinemurian this facies was converted into a deeper water hemipelagic/pelagic basin facies with mixed siliciclastic-carbonate lithologies. This sedimentation was prevailing until Upper Bajocian. The bioturbated hemipelagic/pelagic marl facies ("spotted marl") is characteristic to the European margin of the Tethys (Allgäu facies) (HAAS, 1994).

Stratigraphically, the analysed two profiles represent an Early to Middle Bajocian succession, i. e. upper part of the spotted marl sequence (Komló Calcareous Marl Formation). The Ammonite *Kumatostephanus* sp. indicates the Sauzei Zone (GALÁ CZ, 1997, pers. comm.) found at the base of the section Püspökszentlászló II. (Fig. 2).

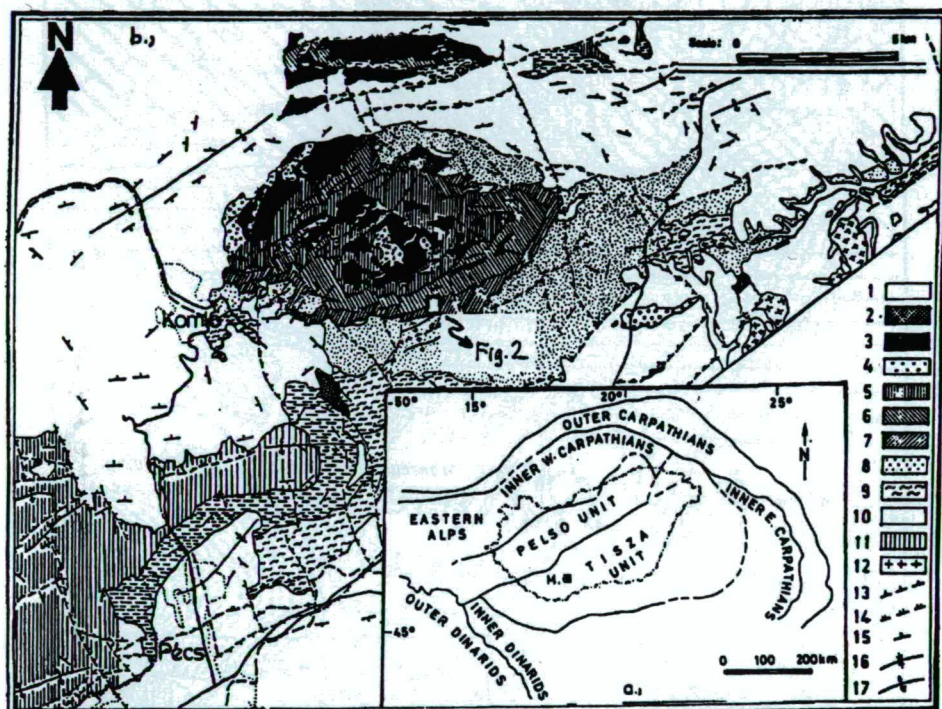


Fig. 1. a) Tectonic position of the Mecsek Mountains (M) in the Alpine-Carpathian system after Haas (1994); b) Geological map of the area simplified after Forgó et al. (1966). 1. Neogene, 2. Lower Cretaceous volcanic rocks, 4. Lower Cretaceous sedimentary rocks, 5. Upper Jurassic, 6. Middle Jurassic, 7. Toarcian, 8. Pliensbachian, 9. Upper Sinemurian, 10. Lower Sinemurian-Hettangian, 11. Triassic, 12. Proterozoic-Early Paleozoic, 13. normal faults, 14. reversed faults, 15. strike and dip of strata, 16. axis of a syncline, 17. axis of an anticline

## PETROGRAPHY

The succession consists of a fairly monotonous alternation of carbonate-poor and carbonate-rich beds. It must be emphasized that in some cases petrographically the same rock types (for example limestones) can exist within a pair of beds but according to field observations those have couplet-like appearance, too. In the Fig. 3 the lithologies are indexed on the base of calcium carbonate content. Their couplet-like appearance is presented by the width of the bed: i. e. wide rectangles of the columns represent the massive,



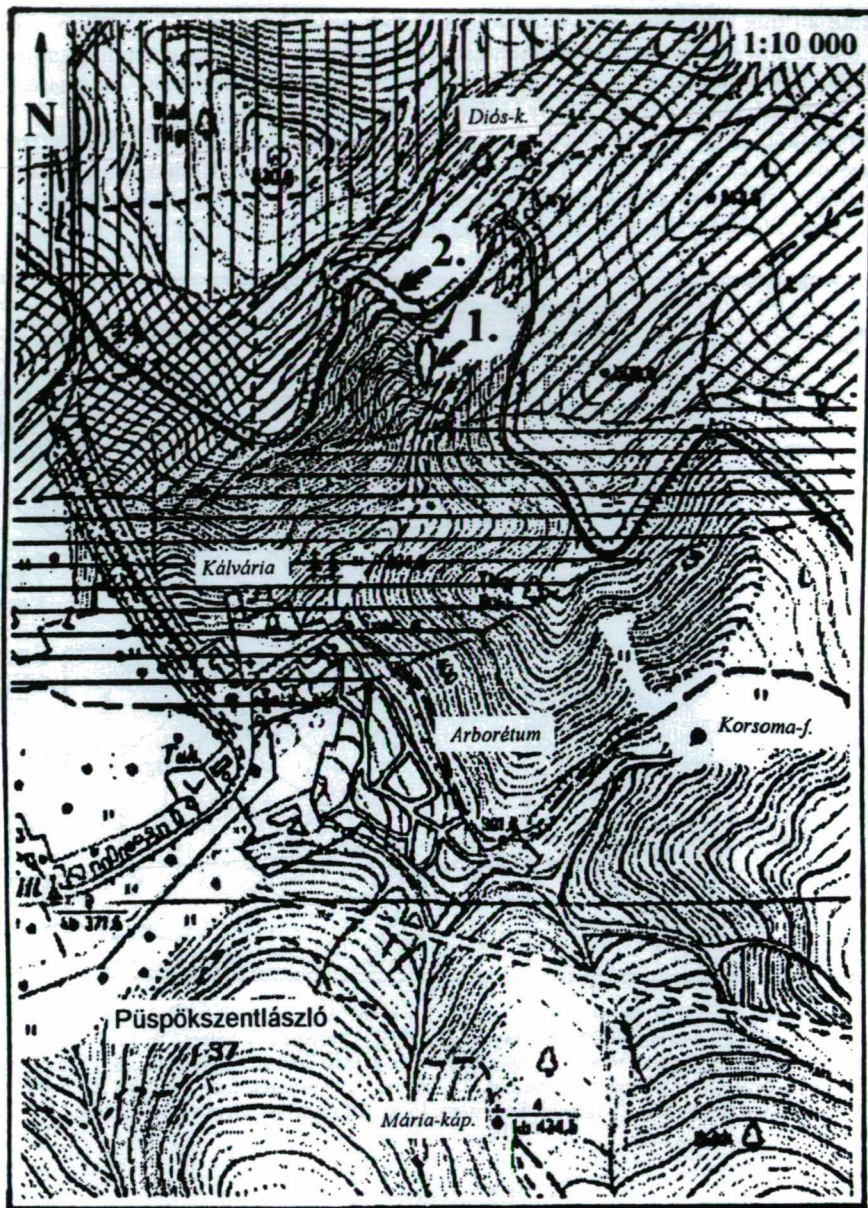






Fig. 2 Locations of the examined sections. 1. Section Püspökszentlászló II., 2. Section Kecsegyúr, road cut

- Legend:
-  Bathonian and younger formations
  -  Komló Calcareous Marl Formation, Bajocian part
  -  Komló Calcareous Marl Formation, Upper Toarcian-Aalenian part
  -  Lower Toarcian and Pliensbachian sediments

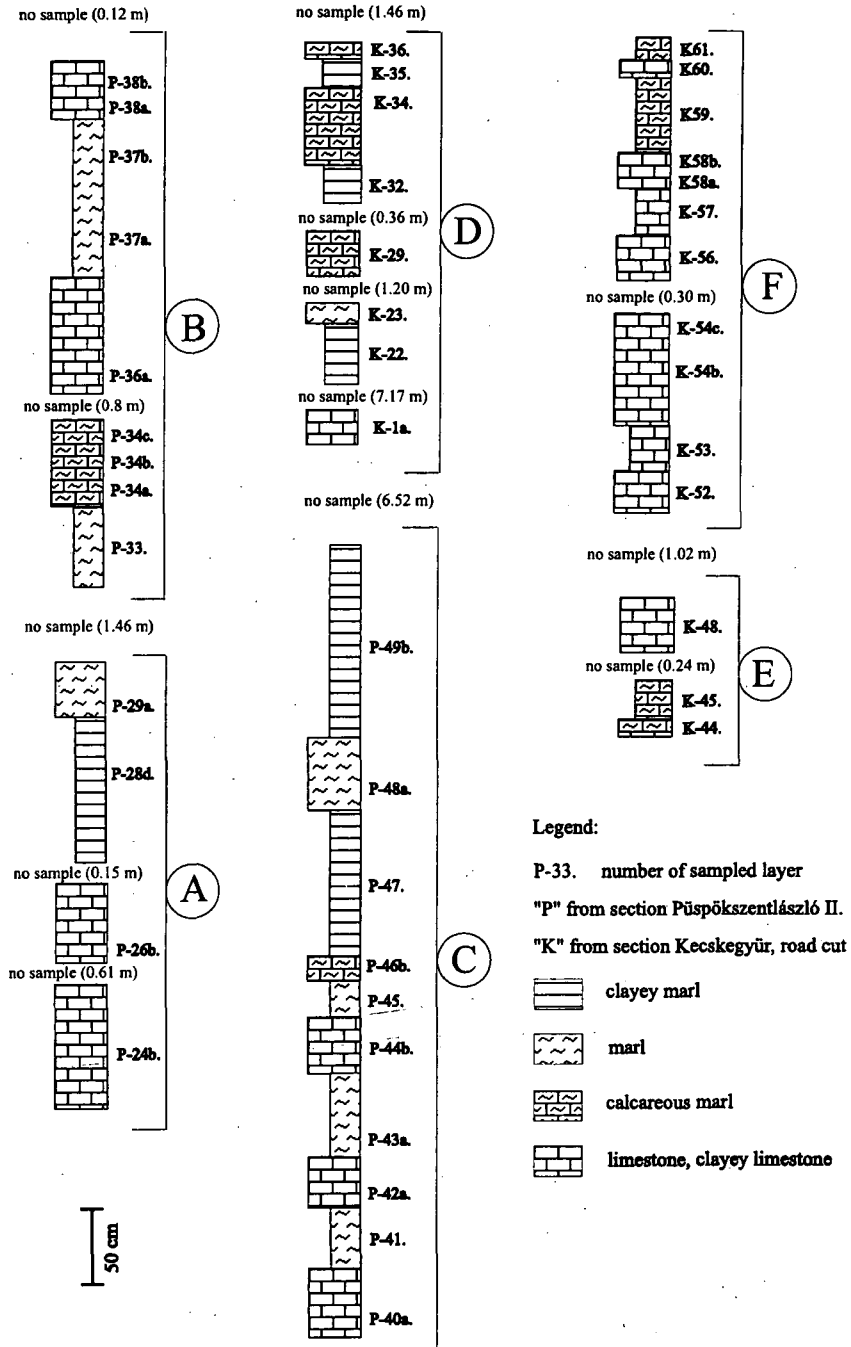


Fig. 3 Lithological column of the examined segments of the sections Püspökszentlászló II. and Kecskegyür, road cut

carbonate-rich semicouplets, whereas the narrower rectangles represent the softer, thin bedded carbonate-poor ones. All of lithology have grey, greenish grey colour, with abundant darker spots. These spots are regarded as product of intensive bioturbation. Intensity of the bioturbation and diversity of the observed ichnofossils, however, fluctuate across the sections. Carbonate-poor beds display poorer ichnofossil assemblage and shallower penetration depth than carbonate-rich layers. These phenomena are interpreted by several worker as product of changing redox conditions (and oxygenation) at the seafloor and/or in sediment mass near the sediment-water interface during sedimentation and early diagenesis (ERBA and PREMOLI SILVA, 1994; SAVRDA and BOTTJER, 1994; SAVRDA, BOTTJER, SEILACHER, 1991). The carbonate-poor beds are slightly darker than the limestones because of their higher clay content. The carbonate-poor beds with the highest clay contents are thin bedded, nevertheless all of the carbonate-rich semicouplets are massive. The CaCO<sub>3</sub> content generally fluctuates between 20-60% for the carbonate-poor beds and increases to 80-98% in the more calcareous layers. The rock types are organized in decimetre-thick couplets. The boundaries between the two dominant lithologies (within a couplet and also between the couplets) are transitional but sharp bedding contact can also be observed. All of these rocks contain quartz and muscovite silt grains with maximum 5% abundance. Rock Eval pyrolysis did not detect significant organic matter (TOC values between 0.04 and 0.17 %, HETÉNYI, 1997, pers. comm.). Because the samples were collected from a surface outcrop, this low organic matter content seems to be, at least partially, result of the oxidation during surface exposure. The above facts and the common presence of limonite pseudomorphs after pyrite besides the absence of lamination suggest that oxic to dysoxic conditions prevailed during deposition of the Komló Calcareous Marl Formation. Sharp bedding contacts may have been developed by erosive sedimentary processes, turbidity and contour current activity (TUCKER and WRIGHT, 1990; PIPER and STOW, 1991). However, another sedimentary structures indicative of redeposition by gravity mass flows (including existence of fine-grained turbidites or contourites), e.g., cross lamination, normal or inverse graded bedding, fine lamination, lenticular bedding, fine, obscure silt lenses, tool marks on underlying bedding planes, complete or incomplete Bouma-sequence were not observed.

In thin section the limestones and marls are classified as bioclastic packstones and wackestones. The most abundant biogene components are radiolarians, siliceous sponges and filaments. Echinoid fragments represent 1-2 percentage of the total bioclast assemblage. Maximum 5% unrounded terrigenous quartz sand and silt grains are present as well. Intensive bioturbation is conspicuous in all samples. Forams (*Lenticulina sp.*, *Spirillina sp.*, *Garantella sp.*) are present in some thin sections, which cannot be used for precise biostratigraphic dating, but they suggest normal marine salinity and deeper shelf area as depositional environment (RESCH, 1997, pers. comm.).

A few marlstone samples show fitted fabric structures. The partial dissolution of some of the biogenic constituents indicate carbonate dissolution and reprecipitation during diagenesis. In outcrops wavy bedding surfaces are widespread; nevertheless carbonate concretions did not form, i.e. carbonate redistribution in the sense of HALLAM (1964) probably was not significant enough to cause this alternation of carbonate-rich and carbonate-poor beds.

The studied profiles represent basinal facies dominated by hemipelagic processes. Sedimentation was presumably continuous. Consequently, this succession is a good object for geochemical analysis to study the origin of Komló Calcareous Marl Formation.

## ANALYTICAL METHODS

The name PIXE (Particle Induced X-Ray Emission) refers to a process in which characteristic X-rays are generated by ion-atom collision events as the consequence of the recombination of electron vacancies appearing in the inner shells. The spectroscopy of X-rays reveals analytical information on the elemental constituents of the samples. In such a way multielemental analysis with low detection limit can be performed on thin and thick samples of small absolute mass (JOHANSSON, 1988).

The 2 MeV energy proton beam of the 5 MeV Van de Graaff accelerator of the Institute of Nuclear Research of the Hungarian Academy of Sciences, in Debrecen has been used for PIXE analysis. Details on the experimental setup and its calibration have been given in BORBÉLY-KISS et al. (1985) as well as in SZABÓ and BORBÉLY-KISS (1993). Powdered samples were pressed into pellets (1 mm thick, 10 mm in diameter). The beam current was typically between 1 and 10 nA, with a beam size of 5 mm diameter, and about 20 minutes bombardment was sufficient to detect elements in the sample. Spectra have been evaluated with the PIXYKLM programme package (SZABÓ and BORBÉLY-KISS, 1993).

Standard deviations given in Table 1a and Table 1b include the statistical errors originating from the measuring conditions and the fitting of X-ray spectra. However, do not include the error of data necessary for the determination of elemental concentrations. Those data (X-ray production cross section, response probability of the Si(Li) detector, X-ray absorption in the sample and in the used filter and the slowing down of proton beam in the sample) are calculated theoretically. Errors of those data are systematic, depend on the atomic number and can only be estimated. They are less than 10-15 % of the value of concentrations.

## RESULTS

Major and trace element data for the samples from six segments (indicated by A-F in Fig. 3) of sections Püspökszentlászló II. and Kecskegyűr, road cut, are listed in Table 1a and 1b. Table 2 shows the main element ratios suggested by the literature. Average values of these elements and element ratios are shown in the Tables 1a, 1b, 2. („average 1.” indicates the calculated average values of the carbonate-rich, „average 2.” indicates those of the carbonate-poor beds.) Values with very high standard deviation are indicated by bold numbers. Correlation matrix is presented in Table 3.

Missing values in the above tables mean that the concentrations of those elements are less than the sensitivity limits.

## DISCUSSION

### *Major elements*

SiO<sub>2</sub> values range from 6.63 (sample P-24b) to 62.69% (sample P-36a). Average value for the carbonate-rich layers is 29.58%, whereas for the carbonate-poor layers it is 48.47%. It is obvious that some limestone layers have higher SiO<sub>2</sub> content than the average value for carbonate-poor semicouplets (P-26b 59.68%, P-34c 49.80%, P-36a 62.69%, K-23 57.54%). The two main sources of Si in these sediments are biogenic opal and aluminosilicate material. Si positively correlates with Ti ( $r=0.700$ ), which indicates dominant terrigenous control on Si distribution. However, according to microfacies observations, many of carbonate-rich samples contain abundant radiolarians. This fact should be the reason for higher SiO<sub>2</sub> content of some carbonate-rich samples.

TABLE 1A

## Major and trace element composition of the measured samples

number of sample	Al <sub>2</sub> O <sub>3</sub> (%)	SiO <sub>2</sub> (%)	CaO (%)	K <sub>2</sub> O (ppm)	TiO <sub>2</sub> (ppm)	MnO (ppm)	Fe <sub>tot</sub> (ppm)
P-24b	3.63±0.7	6.63±0.3	55.25±2.2	3134±300	445±150	262±30	6910±290
P-26b	5.74±0.8	59.68±2.4	18.33±0.7	11081±500	1269±610	188±30	10820±450
P-28d	3.29±0.8	54.97±2.2	22.43±0.9	9359±440	1495±130	194±30	10340±430
P-29a	3.36±0.7	43.10±1.7	27.98±1.1	6138±330	1281±140	247±50	8478±360
P-33	5.63±0.8	51.08±0.5	24.69±1.0	10754±490	1676±140	214±30	12390±510
P-34a	0.76±0.7	18.72±0.5	45.50±1.8	4813±290	787±130	258±30	7719±320
P-34b	3.29±0.7	8.56±0.4	52.27±2.1	2944±270	754±140	235±30	7241±300
P-34c	5.63±0.7	49.80±1.9	28.06±1.1	8983±430	1349±130	203±30	6964±290
P-36a	37.79±2.0	62.69±2.5	29.02±1.1	7545±380	1274±120	141±20	5879±250
P-37a	12.89±0.9	57.62±2.3	13.64±0.5	20585±870	3521±900	250±40	16320±670
P-37b	5.48±0.9	47.83±1.9	26.06±1.0	12628±570	2082±160	216±30	12140±500
P-38a	1.10±0.8	19.94±0.8	46.91±1.9	4999±340	914±160	217±30	6815±280
P-38b	1.93±0.7	11.89±0.5	50.48±2.0	5307±320	1000±140	239±30	6898±290
P-40a	2.87±0.7	29.15±1.2	38.18±1.5	5594±330	1098±130	178±30	8380±350
P-41	6.61±0.9	49.00±2.0	25.21±1.0	13881±610	2345±170	221±30	12590±520
P-42a	4.61±0.7	16.17±0.7	46.89±1.9	4259±300	736±130	225±30	7227±300
P-43a	9.64±0.8	53.77±2.8	17.80±0.7	17046±730	2705±170	200±30	16390±670
P-44b	1.70±0.8	9.05±0.4	53.43±2.1	4331±300	1161±210	488±50	8473±350
P-45	8.50±0.9	48.11±2.0	24.92±1.0	14695±650	2562±180	234±30	13310±550
P-46b	2.76±0.7	26.59±1.1	42.39±1.7	6302±350	1106±150	214±30	8071±330
P-47	7.71±0.9	57.37±2.3	15.49±0.6	19696±830	3283±190	227±30	15380±630
P-48a	4.27±0.7	47.93±1.9	28.62±1.1	7740±400	1503±140	196±30	9801±400
P-49b	5.06±0.6	45.75±1.9	29.91±1.2	8159±410	1434±140	188±30	9088±380
K-1a	2.42±0.8	13.80±0.6	51.89±2.1	3006±280	257±140	638±50	5124±220
K-22	6.20±0.8	44.17±1.8	29.92±1.2	11941±550	1613±140	296±40	10630±440
K-23	13.79±1.0	57.54±2.3	16.45±0.7	23562±980	3178±190	247±40	16210±670
K-29	6.24±0.8	40.83±1.7	31.62±1.3	12838±580	1693±150	359±40	9626±400
K-32	6.92±0.9	46.84±1.9	21.03±0.8	25150±1050	3026±190	258±40	17020±700
K-34	4.35±0.7	40.28±1.6	29.67±1.2	15750±680	2115±160	332±40	11580±480
K-35	4.27±0.8	47.55±1.9	22.47±0.9	23160±970	2782±190	235±40	15270±630
K-36	1.36±0.8	23.57±1.0	43.33±1.7	6574±360	812±140	318±40	8543±360
K-44	3.78±0.7	37.05±1.5	29.39±1.2	18489±790	2278±170	376±40	13370±550
K-45	8.05±0.7	38.91±1.6	27.67±1.1	20956±890	2741±190	341±40	13930±570
K-48	4.16±0.7	9.15±0.4	49.65±2.0	3341±270	350±130	385±40	4045±170
K-52	4.16±0.9	11.74±0.5	51.65±2.1	3573±280	425±130	542±40	5904±250
K-53	9.11±0.9	45.73±1.9	22.66±0.9	23719±1000	2976±190	372±40	16400±670
K-54b	0.76±0.8	27.57±1.1	41.75±1.7	6798±370	652±130	528±50	6584±280
K-54c	5.18±0.8	23.14±1.0	43.15±1.7	5558±330	637±120	580±50	7669±320
K-56	5.03±0.8	31.25±1.3	37.02±1.5	7969±400	1059±120	452±40	6927±290
K-57	11.79±0.8	43.59±1.8	23.53±0.9	26740±1120	3256±200	381±40	16010±660
K-58a	1.02±0.9	33.20±1.4	38.58±1.6	9732±470	1178±150	553±40	8507±350
K-58b	6.20±0.8	40.21±1.6	29.63±1.2	14334±630	1908±160	520±50	15830±650
K-59	12.40±0.9	47.10±1.9	20.45±0.8	34280±1420	4078±240	435±40	20160±820
K-60	3.67±0.9	28.92±1.2	40.33±1.6	9583±470	1291±150	600±50	8860±370
K-61	11.71±0.9	40.71±1.7	27.06±1.1	24138±1010	2757±190	524±50	14970±610
average 1.	5.06±0.8	29.58±1.2	39.20±1.6	8010±400	1124±160	347±40	8516±350
average 2.	7.94±0.8	48.47±1.9	23.24±0.9	17550±800	2607±220	288±40	14255±560



TABLE 1B

## Major and trace element composition of the measured samples

number of sample	Rb (ppm)	Sr (ppm)	V (ppm)	P (ppm)	Ni (ppm)	Cu (ppm)	Zn (ppm)
P-24b	-	735±50	-	6303±410	-	-	14±6
P-26b	44±13	424±40	-	-	-	22±6	43±6
P-28d	45±17	500±50	-	-	-	20±7	36±7
P-29a	35±16	589±50	-	1966±520	-	-	27±10
P-33	<b>26±13</b>	<b>468±40</b>	-	<b>1012±550</b>	-	17±6	53±7
P-34a	31±14	721±50	-	5924±410	-	11±5	50±7
P-34b	40±15	862±50	-	5593±370	-	14±5	22±6
P-34c	29±13	464±40	98±45	3323±600	-	16±6	35±6
P-36a	<b>19±12</b>	449±40	<b>76±43</b>	3584±650	-	23±6	30±6
P-37a	47±13	190±30	-	1730±640	<b>31±16</b>	30±7	55±8
P-37b	36±14	420±40	104±54	2705±590	-	20±6	50±7
P-38a	44±14	692±50	-	5452±490	-	<b>12±6</b>	24±6
P-38b	37±14	700±50	-	6618±440	-	15±6	28±6
P-40a	41±14	563±40	-	3464±480	-	16±6	34±6
P-41	41±14	390±40	144±55	1750±570	-	17±6	51±8
P-42a	54±15	742±50	<b>90±53</b>	5126±420	-	<b>12±6</b>	21±6
P-43a	41±13	308±30	-	2278±580	<b>24±16</b>	24±6	67±8
P-44b	43±14	724±50	-	8739±550	<b>20±12</b>	14±6	24±6
P-45	40±13	335±30	-	2169±560	-	22±7	54±8
P-46b	43±12	586±40	-	4788±500	-	11±5	28±6
P-47	51±13	247±30	157±56	-	-	16±6	68±8
P-48a	40±14	534±40	137±45	2103±560	-	21±6	29±6
P-49b	35±14	471±40	-	2927±560	-	20±6	44±7
K-1a	25±11	377±30	-	8027±500	-	<b>11±6</b>	15±5
K-22	46±15	420±40	-	1914±540	-	20±7	46±8
K-23	52±15	225±30	121±53	-	<b>26±16</b>	23±7	62±8
K-29	52±14	376±40	-	2723±550	<b>24±13</b>	19±7	42±7
K-32	56±15	261±30	131±59	-	-	25±7	75±9
K-34	41±15	368±40	-	2762±530	<b>29±15</b>	19±7	52±8
K-35	38±14	259±30	-	2144±580	<b>28±16</b>	21±7	69±9
K-36	44±15	534±40	-	5404±490	<b>22±12</b>	15±6	37±7
K-44	55±15	284±30	<b>107±57</b>	3123±500	31±15	25±7	58±8
K-45	57±16	269±30	<b>107±59</b>	1883±510	31±15	23±7	68±8
K-48	<b>22±13</b>	488±40	-	7083±430	-	<b>10±6</b>	14±6
K-52	<b>19±13</b>	491±40	-	6880±460	-	14±6	20±6
K-53	56±15	263±30	176±60	1334±600	<b>30±16</b>	16±7	87±9
K-54b	40±12	378±30	-	6536±520	-	-	17±6
K-54c	28±13	447±40	-	6919±490	<b>19±11</b>	<b>10±6</b>	33±6
K-56	<b>25±12</b>	383±30	84±41	5025±490	<b>20±11</b>	14±5	27±6
K-57	58±15	281±30	141±60	3877±540	32±16	25±7	83±9
K-58a	34±12	397±30	-	5720±560	23±11	13±6	29±6
K-58b	37±13	306±30	<b>102±55</b>	4722±550	<b>26±15</b>	15±6	53±7
K-59	54±15	197±30	137±67	3363±550	41±18	26±7	102±10
K-60	36±12	373±30	-	5984±530	<b>19±12</b>	<b>12±6</b>	35±6
K-61	54±15	277±30	-	4904±540	32±15	21±7	62±8
average 1.	36±13	508±40	102±50	5150±500	<b>24±13</b>	15±6	32±6
average 2.	45±14	321±30	137±60	2428±560	<b>31±16</b>	21±7	63±8

TABLE 2

*The applied element-ratios*

number of sample	Si/Al	Al/(Al+Fe+Mn)	Fe/Ti	Fe/Mn	Mn/Ti	P/Ti	Sr/Ti
P-24b	3.24	0.15	25.87	34.09	0.76	23.60	2.75
P-26b	18.40	0.30	14.21	73.96	0.19	-	0.56
P-28d	29.64	0.27	11.54	69.12	0.17	-	0.56
P-29a	22.69	0.23	11.04	44.41	0.25	2.56	0.77
P-33	16.05	0.26	12.33	74.82	0.16	1.01	0.47
P-34a	44.37	0.20	16.34	38.63	0.42	12.54	1.53
P-34b	4.60	0.14	16.02	39.90	0.40	12.38	1.91
P-34c	15.66	0.34	8.61	44.30	0.19	4.11	0.57
P-36a	2.93	0.34	7.70	54.13	0.14	4.69	0.59
P-37a	7.91	0.05	7.73	84.04	0.09	0.82	0.09
P-37b	15.38	0.30	9.73	72.52	0.13	2.17	0.34
P-38a	32.28	0.23	12.44	40.61	0.31	9.95	1.26
P-38b	10.81	0.24	11.51	37.31	0.31	11.05	1.17
P-40a	17.90	0.21	12.73	60.81	0.21	5.26	0.86
P-41	13.12	0.31	8.95	73.67	0.12	1.24	0.28
P-42a	6.19	0.19	16.39	41.53	0.39	11.62	1.68
P-43a	9.86	0.30	10.10	105.47	0.06	1.40	0.19
P-44b	9.36	0.17	12.17	22.41	0.54	12.55	1.04
P-45	9.98	0.31	8.67	73.50	0.18	1.41	0.22
P-46b	17.04	0.24	12.18	48.68	0.25	7.22	0.88
P-47	13.17	0.34	7.82	87.64	0.09	-	0.13
P-48a	19.87	0.24	10.88	64.65	0.17	2.34	0.59
P-49b	16.02	0.27	10.57	62.33	0.17	3.41	0.55
K-1a	10.04	0.18	33.25	10.37	3.21	52.09	2.45
K-22	12.61	0.31	10.99	46.46	0.24	1.98	0.44
K-23	7.37	0.37	8.51	84.69	0.10	-	0.12
K-29	11.59	0.35	9.48	34.65	0.27	2.68	0.37
K-32	11.94	0.38	9.38	85.06	0.11	-	0.14
K-34	16.40	0.36	9.13	45.06	0.20	2.17	0.29
K-35	19.62	0.38	9.15	58.87	0.16	1.26	0.16
K-36	30.62	0.24	17.56	34.69	0.51	11.11	1.10
K-44	17.36	0.36	9.79	46.15	0.21	2.29	0.21
K-45	8.52	0.38	8.48	52.73	0.16	1.15	0.16
K-48	3.91	0.24	19.24	13.57	1.42	33.70	2.32
K-52	5.00	0.19	23.11	14.07	1.64	26.94	1.92
K-53	8.87	0.37	9.19	57.00	0.16	0.75	0.15
K-54b	63.59	0.29	16.86	16.11	1.05	16.73	0.99
K-54c	7.87	0.22	20.10	17.08	1.18	18.13	1.17
K-56	10.96	0.31	10.91	19.80	0.55	7.92	0.60
K-57	6.54	0.41	8.20	54.22	0.15	1.99	0.14
K-58a	57.57	0.31	12.05	19.86	0.61	8.10	0.56
K-58b	11.46	0.27	13.84	39.31	0.35	4.13	0.27
K-59	6.71	0.41	8.25	59.89	0.14	1.38	0.08
K-60	13.96	0.30	11.45	19.06	0.60	7.73	0.48
K-61	6.14	0.39	9.06	36.87	0.25	2.97	0.17
average 1.	17.61	0.26	26.24	35.92	1.21	25.60	2.13
average 2.	12.48	0.32	9.42	67.89	0.15	1.35	0.25

TABLE 3

## Correlation matrix

Elements and element-ratios	Al	Si	P	K	Ca	Ti	V	Mn	Fe	Ni	Cu	Zn	Rb	Sr	Si/Al	Al/(Al+Fe+Mn)	Fe/Ti	Fe/Mn	Mn/Ti	P/Ti	Sr/Ti	$\delta^{13}\text{C}$	$\delta^{18}\text{O}$
Al	1	0.544	-0.326	0.384	-0.449	0.414	-0.233	-0.213	0.290	0.615	0.523	0.332	0.009	-0.383	-0.429	0.337	-0.387	0.346	-0.266	-0.279	-0.351	-0.729	-0.485
Si		1	-0.851	0.625	-0.959	0.700	0.301	-0.397	0.645	-0.587	0.734	0.617	0.269	-0.670	-0.042	0.546	-0.702	0.762	-0.589	-0.730	-0.830	-0.806	-0.819
P			1	-0.567	0.870	-0.679	-0.659	-0.552	-0.623	-0.619	-0.695	-0.616	-0.344	0.470	0.121	-0.424	0.686	-0.806	0.672	0.768	0.720	0.604	0.848
K				1	-0.773	0.956	0.610	0.024	0.935	0.912	0.725	-0.940	0.664	-0.809	-0.185	0.853	-0.613	0.457	-0.459	-0.572	-0.755	-0.772	-0.406
Ca					1	-0.835	-0.654	0.338	-0.801	-0.686	-0.786	-0.761	-0.433	0.751	0.097	-0.572	0.721	-0.806	0.608	0.751	0.864	0.857	0.764
Ti						1	0.707	-0.144	0.952	0.870	0.769	0.920	0.652	-0.755	-0.261	0.580	-0.713	0.690	-0.569	-0.680	-0.805	-0.801	-0.520
V							1	0.061	0.676	0.512	0.103	-0.685	0.599	-0.473	0.138	0.357	-0.227	0.57	-0.551	-0.656	-0.524	-0.633	-0.322
Mn								1	-0.076	-0.314	-0.332	-0.082	-0.113	-0.256	0.089	0.048	0.401	-0.706	0.625	0.450	0.156	-0.022	0.483
Fe									1	0.830	-0.709	0.932	-0.628	-0.725	-0.219	0.530	-0.592	0.683	-0.530	-0.634	-0.763	-0.826	-0.496
Ni										1	0.772	0.871	0.725	-0.694	-0.274	0.433	-0.645	0.476	-0.715	-0.750	-0.745	-0.600	0.015
Cu											1	0.654	0.494	-0.608	-0.234	0.405	-0.621	0.681	-0.360	-0.612	-0.711	-0.624	-0.545
Zn												1	0.614	-0.708	-0.203	0.662	-0.609	0.607	-0.532	-0.617	-0.747	-0.732	-0.472
Rb													1	-0.325	-0.081	0.383	-0.483	0.370	-0.497	-0.496	-0.525	-0.504	-0.390
Sr														1	0.113	-0.643	0.148	-0.366	0.130	0.313	0.708	0.830	0.311
Si/Al															1	-0.022	0.036	-0.181	0.013	-0.023	-0.020	0.066	0.055
Al/(Al+Fe+Mn)																1	-0.573	0.253	-0.377	-0.476	-0.666	-0.711	-0.469
Fe/Ti																	1	-0.586	0.875	0.925	0.879	0.552	0.626
Fe/Mn																		1	-0.657	-0.667	-0.605	-0.632	-0.700
Mn/Ti																			1	0.949	0.704	0.378	0.622
P/Ti																				1	-0.864	0.510	0.758
Sr/Ti																					1	0.783	0.698
$\delta^{13}\text{C}$																						1	0.560
$\delta^{18}\text{O}$																							1

Al<sub>2</sub>O<sub>3</sub> values fluctuate from 0.76 (samples P-34a and K-54b) to 37.79% (sample P-36a). The average for the carbonate-rich semicouplets is 5.06%, for the carbonate-poor semicouplets is 7.94%, correlating with the clay mineral abundance of the given samples. Two carbonate-rich samples show obviously high Al<sub>2</sub>O<sub>3</sub> content (P-36a 37.79%, K-23 13.79%). It must be emphasized, that six Al<sub>2</sub>O<sub>3</sub> values of the 45 are not accurate enough to use. Therefore these values must be use with caution. TiO<sub>2</sub> values vary between 257 ppm (K-1a) and 4078 ppm (K-59). Average values are 1124 and 2607 ppm for the carbonate-rich and the carbonate-poor semicouplets, respectively. Three TiO<sub>2</sub> values are not available.

Aluminium or titanium normalizations are generally used to correct for the terrestrial influences in marine sediments (MURRAY et al., 1991, 1993, MURRAY and LEINEN, 1996, NATH et al., 1992). In CaCO<sub>3</sub>-rich biogenic sediments, a portion of Al may be affiliated by adsorption processes to biogenic fraction (MURRAY et al., 1993, MURRAY and LEINEN, 1996, SCHROEDER et al., 1997), thus Al normalization does not seem to be optimal in this case. Similarly, the Al/(Al+Fe+Mn) ratio (proposed by BELLANCA et al., 1996) must be used with caution for estimating the terrigenous supply. Unlike Al, no proven biological affiliation is reported for Ti, therefore this element is used for normalization and to represent the terrigenous siliciclastic component of bulk sediment.

CaO values depend strictly on calcite content of the samples. The highest value is 55.25% (P-24b), the lowest is 13.64% (P-37a). Average value for the carbonate-rich semicouplets is 39.20%, for the carbonate-poor semicouplets is 23.24%.

K<sub>2</sub>O data fluctuate from 2944 (P-34b) to 34280 ppm (K-59). Main values are 8010 and 17550 ppm for the calcite-rich and the calcite-poor semicouplets, respectively. This suggests a major role of the silicate minerals in the K<sub>2</sub>O distribution.

Fe<sub>TOT</sub> values fluctuate from 4045 (K-48) to 20160 ppm (K-59). Average value for calcite-rich beds is 8516 ppm, for calcite-poor beds is 14255 ppm. Fe values show excellent correlation with Ti ( $r=0.952$ ) and K ( $r=0.935$ ). Fe values plotted versus Ti represent a good agreement with values characteristic of average shale, which indicates that all the three elements are derived primarily from lithogenic source. Concentrations of Fe when plotted against Ti, fall over the line representing the trend for average shale (Fig. 4). (In Figs. 4; 7; 8; 9; 10; 11 solid line represents the element/Ti ratios in average shale according to TUREKIAN (1972)). Nevertheless, the Fe/Ti ratio correlates with the Ca ( $r=0.721$ ) and shows in many cases significant excess Fe corresponding with PAAS (Post-Archaean Australian Shale, values from TAYLOR and MCLENNAN, 1985) (Fig. 5). The Ti-normalized enrichments with respect to PAAS indicates the presence of chemical sources in addition to the lattice-bound aluminosilicate contribution to the sediment (MURRAY and LEINEN, 1993). This suggests some amount of excess (non-detrital) Fe links to the abundant carbonate component of the examined rocks. The Fe enrichment in the marly intervals coupled with the presence of some pyrite pseudomorphs and moderate bioturbation reflect a poorly-oxigenated environment and a wide availability of reactive iron for authigenic mineral formation. The correlation of iron and titanium testifies that the amounts of Fe incorporated in sediments were largely controlled by detrital iron-bearing minerals. Moderate diagenetically-controlled Fe enrichment, however, cannot be excluded.

### *Trace elements*

Trace elements in sediments that accumulate on the seafloor have two sources: detrital clastic detritus and seawater (KUMAR et al., 1996). The seawater-derived fraction also has



two components: a portion that is incorporated into the marine organisms and a component that is scavenged from the dissolved elemental load of seawater by organic and inorganic particles settling through the water column.

Relations of trace elements to Ti defined for average shale, as stated above, seems to be available tool to estimate excess amounts (over detrital) of trace element. Ni (*Fig. 7*) shows relatively good accordance with the trend line characteristic of average shale, as well as the correlation between of Ni and Ti is good ( $r=0.870$ ). Many workers give account of lower redox-sensitivity of Ni relative to other elements, above all to V (ODERMATT and CURIALE, 1991; HUERTA-DIAZ and MORSE, 1992). These features suggest that the main source of Ni is the terrigenous fraction; direct or biogenic-controlled seawater source of Ni are not provable on the basis of these data. Cu (*Fig. 8*), Zn (*Fig. 9*), V (*Fig. 10*) and Sr (*Fig. 11*) values, however, are much higher than in average shale. According to these patterns one should take into account significant amount of excess (over detrital) trace metal content, which probably derived (directly or indirectly) from seawater.

Vanadium fluctuates through the section exhibiting low values for limestones (mean value: 102 ppm) and slightly higher values in the marly intervals (mean value: 137 ppm). The amount of other trace metals (Cu, Zn) fluctuates in a similar manner showing an enrichment in the marly intervals (*Fig. 12*). Vanadium values correlate neither with Al ( $r=-0.233$ ) nor with  $Al/(Al+Fe+Mn)$  ratio ( $r=0.357$ ) but show positive correlation with Ti values ( $r=0.707$ ). V plotted against Ti indicates excess amount of V corresponding to average shale, suggesting that the affiliation with the aluminosilicates is not exclusive control on the V concentration in marlstones of the studied sections. Vanadium solubility in natural waters, its precipitation from seawater and addition to sediments are controlled by redox conditions and by absorption and complexation processes. Dissolved vanadium can be strongly bound to metallo-organic complexes (LEWAN and MAYNARD, 1982) or adsorbed on biogenic particles (PRANGE and KREMLING, 1985). Adsorption and complexation of vanadium are enhanced in anoxic environments where vanadium is present as a reduced V (IV) species. During post-depositional and diagenetic alteration of sediments, vanadium can be mobilized from degrading biogenic particles under oxic conditions, while it is less mobile in disoxic and anoxic sediments. Also V, together with Cu and Zn, is enriched under disoxic conditions, where these metals are trapped with organic material (SHAW et al., 1990; HATCH and LEVENTHAL, 1992). However, it must be emphasized, that in this case the use of the  $V/(V+Ni)$  ratio as a tool for proxy of redox conditions (LEWAN, 1984; HATCH and LEVENTHAL, 1992) is not favorable because of the limited number of accurate V (13 samples show enough amount of V) and Ni (six samples with sufficient accuracy for Ni) data. Using Zn and Cu values seems better.

The data indicate that the Zn concentration (up to 102 ppm) is about 1.5-2 times the amount can be explained from an aluminosilicate source. Organic matter derived from plankton with average concentrations of Zn is 110 ppm (DEAN et al., 1997). Excess (over detrital) concentrations of other chalcophile elements such as Cu (up to 30 ppm) may also be in sulfides, but more likely, the excess amounts are associated with the organic fraction, either as metal-organic complexes (BRULAND, 1983) or adsorbed on organic coatings in particulate organic matter (BALISTRIERI et al., 1981). The stratigraphic distribution of the Zn and Cu values shows differences in metal concentrations within each lithological couplet (*Fig. 12*). This pattern implies the occurrence of fluctuations in the redox state of the depositional environment of the studied section, therefore during more oxygenated periods of sedimentation (represented by carbonate-rich semicouplets) these organo-metal

complexes oxidized then mobilized and migrated in the sediment. During periods characterized by less oxygenated and, probably, disoxic seafloor (represented by carbonate-poor semicouplets) these metal ions and organo-metal complexes could remain in reduced, consequently less mobile state. In the case of Zn it must be emphasized that this metal shows excellent correlation with Ti ( $r=0.920$ ), thus its fluctuating distribution through the section can be explained, partially, by fluctuating terrigenous (also clay mineral) supply. However, the relationships between Ti and Zn abundances suggest some redox-controlled diagenetic redistribution.

Compared to PAAS all these Bajocian sediments from the Mecsek Mountains have low Rb (Rb values fluctuate between 19 and 58 ppm; averages for carbonate-rich semicouplets=36 ppm, for carbonate-poor semicouplets=45 ppm; Rb in PAAS=80 ppm) and high Sr (Sr values vary from 190 to 862 ppm; averages for carbonate rich-semicouplets=508 ppm, for carbonate-poor semicouplets=321 ppm; Sr in PAAS=160 ppm) abundances. The incorporation of Sr into the crystal structure of calcite, expressed by the Sr/Ti ratio, explains the excess concentrations of this element in carbonate-rich sediments (*Fig. 13*).

MnO values fluctuate between 141 and 638 ppm. The mean MnO value for carbonate-rich layers (347 ppm) is significantly higher than for carbonate-poor semicouplets (288 ppm). The high sensitivity of manganese to environmental redox conditions is well known (FORCE and CANNON, 1988; SAAGER et al., 1989; GOBEIL et al., 1997). In hemipelagic sediments subjected to a transition from suboxic (or anoxic) to oxic conditions, low Eh conditions can lead to a Mn enrichment in the porewater and the subsequent upward diffusion of dissolved Mn may concentrate this element in the solid phase, just above or below the redox boundary. DICKENS and OWEN (1994) have suggested that the redox-sensitive Mn oxo-hydroxide particulates dissolve upon entering an oxygen minimum zone. The resulting  $Mn^{2+}$  is subsequently redirected by advective and/or diffusive processes eventually to precipitate in more oxygenated environments. Thus, the fluctuation of Mn values may be interpreted as an indicator of rhythmic changes in sedimentary redox conditions. The record of Mn should reflect migration of the metal from weaker oxic clay-rich layers and concentrations of the same metal in more oxygenated carbonate-rich layers, where it is incorporated in the carbonate phase and/or precipitated as oxide, oxo-hydroxide coatings on biogenic tests.

The differences in the solubility of reduced iron and manganese could lead to sedimentary fractionation of these elements across redox boundaries. Large portion of iron being fixed in sulphide under low Eh conditions (SAAGER et al., 1989). The Mn/Ti profile shows fluctuations generally opposite to those of Ti (*Fig. 14a*) and parallel to those of Ca (*Fig. 14b*). The high Fe/Mn values indicate, according to MACHOUR et al. (1994), mildly to strongly reducing conditions during deposition. The Fe/Mn index increases systematically from the carbonate-rich to the clay-rich part of each lithological couplet (*Fig. 15*) outlining variations in the redox-state of the bottom-waters in the Bajocian basin of Mecsek Mountains.

Phosphorous values have a minimum of 1012 ppm (P-33) and a maximum of 8739 ppm (P-44b). Average values are 5150 and 2428 ppm for the calcite-rich and the calcite-poor semicouplets, respectively. One result ( $1012 \pm 550$  ppm, sample P-33) is just informative.

P, Sr and Ba in marine sediment and biogenic particulate matter are commonly affiliated with biogenic phases (FROELICH et al., 1982; FISHER et al., 1991; PINGITORE et al., 1992; MURRAY and LEINEN, 1993) and as such are commonly enriched in sediment

deposited beneath productive surface waters (GOLDBERG and ARRHENIUS, 1958; FROELICH et al., 1982; BISHOP, 1988; FISHER et al., 1991). Efforts have capitalized on this relationship in order to assess paleoproductivity from within the marine stratigraphic record. P correlates well with Ca ( $r=0.870$ ) and negatively with the terrigenous influx indicating elements (Ti:  $r=-0.679$ , Si:  $r=-0.851$ ). According to P/Ti ratios (Fig. 6) just a small part of the P in the bulk sediment may be explained by the adsorption onto terrigenous phases (clay minerals); a significant portion seems to be connected to disseminated apatite-group phases, which originally incorporated into the siliceous and carbonate skeleton of organisms (BISHOP, 1988). The transporting agents (opal and calcite) partially degraded on the seafloor, leaving behind the P record as a dissolution residue (FROELICH et al., 1982; MURRAY and LEINEN, 1993). This should indicate enhanced productivity during deposition of the carbonate-rich layers.

According to the interpretation of RAUCSIK (1997) surface seawater should be more saline and/or cooler during deposition of the carbonate-rich semicouplets corresponding to carbonate-poor semicouplets, on the base of the  $\delta^{18}\text{O}$  values. The  $\delta^{13}\text{C}$  values suggest enhanced productivity during deposition of carbonate-rich beds. Carbonate-poor beds seem to be deposited during periods of moderate surface water productivity. Alternating anti-estuarine and estuarine circulation in the basin was proposed as driving force on sedimentation.

## SUMMARY AND CONCLUSIONS

The results of petrographical and geochemical studies coupled with data of formerly stable isotope measurements (RAUCSIK, 1997) are the following:

1. High concentrations of the trace elements such as Mn, Zn, Cu, V and Sr in the samples cannot be explained by a pure detrital clastic source. Excess concentrations (over detrital) of these trace elements may be derived from seawater and are probably associated with the organic fraction.

2. The limestone semicouplets are characterized by good oxygenation as expressed by the pervasive bioturbation, by the Fe/Mn parameter and by the lack of preserved organic matter. The abundance of silica in the absence of high terrigenous input suggests that during limestone deposition surface waters were rather highly fertile due to an efficient recycling of nutrients from deeper waters. The enhanced fertility was coupled with a current system at the well-oxygenated seafloor which prevented the accumulation of organic matter and the trace elements bound by organic matter, such as Zn, Cu and V. During early diagenesis Mn should have migrated from weaker oxic parts of sediment and precipitated as carbonate and/or as oxide, oxi-hydroxide coatings on biogenic tests resulting Mn-enrichment in the carbonate-rich semicouplets. Highly fertile conditions are expressed by  $\delta^{13}\text{C}$  values and Sr- and P-enrichment during deposition of carbonate-rich semicouplets. All parameters indicate high fertility in surface waters caused by increased upwelling that engendered high nutrient levels in near-surface waters.

3. The marly semicouplets deposited under moderately oxic, probably dysoxic conditions (indicated by the Fe/Mn parameter), which not allowed the preservation of abundant organic matter and the appearance of sedimentary structure such as lamination. High  $\text{TiO}_2$  and  $\text{SiO}_2$  values indicate that marly semicouplets received a substantial contribution from a terrigenous source. High Fe values of carbonate-poor layers seems to be affiliated to the enhanced terrigenous supply. However, the differences in the solubility

of reduced iron and manganese could lead to sedimentary fractionation of these elements across redox boundaries and could result in a slight Fe-enrichment during deposition of carbonate-poor semicouplets. Trace metals such as Zn, Cu and V were carried as organo-metal complexes and as adsorbed ions on clay minerals in the water column. Disoxic conditions in the sediment mass and at the seafloor were favorable to preservation and accumulation of these trace elements. On the base of formerly stable carbon isotope measurements, the depositional environment can be characterized by lower surface-water fertility and productivity during deposition of marly beds.

4. The rhythmic organization of couplets should represent climatic changes. Palaeoceanographic conditions alternated from efficiently mixed, highly-fertile surface waters and well-oxygenated seafloor, to enhanced water runoff and/or decreased evaporation and moderately oxygenated bottom waters. The presence of less saline, <sup>18</sup>O-depleted surface-waters may have created stratification that caused moderately oxidizing (most likely dysoxic) conditions at the bottom. The corresponding climatic conditions thus alternated from more arid to more humid.

#### ACKNOWLEDGEMENT

The authors are indebted to ERNŐ MÉSZÁROS, University of Veszprém, for making the measurements possible.

#### REFERENCES

- BALÁZS, E., CSEREPES-MESZÉNA, B., NUSSZER, A., SZILI, GY., GYÉMÁNT, P. (1986): An attempt to correlate the metamorphic formations of the Great Hungarian Plain and the Transylvanian Central Mountains (Muntii Apuseni). *Acta Geol. Hung.* 29., 317-320.
- BALISTRERI, L., BREWER, P. G., MURRAY, J. W. (1981): Scavenging residence times of trace metals and surface chemistry of sinking particles in the deep ocean. *Deep-Sea Res.* 28., 101-121.
- BELLANCA, A., CLAPS, M., ERBA, E., MASETTI, D., NERI, R., PREMOLI SILVA, I., VENEZIA, F. (1996): Orbitally induced limestone/marlstone rhythms in the Albian-Cenomanian Cison section (Venetian region, northern Italy): sedimentology, calcareous and siliceous plankton distribution, elemental and isotope geochemistry. *Palaeogeogr., Palaeoclim., Palaeoecol.* 126., 227-260.
- BICKERT, T., PATZOLD, J., SAMTLEBEN, C., MUNNECKE, A. (1997): Palaeoenvironmental changes in the Silurian indicated by stable isotopes in brachiopod shells from Gotland, Sweden. *Geochim. Cosmochim. Acta* 61/13., 2717-2730.
- BISHOP, J. K. B. (1988): The barite-opal-organic carbon association in oceanic particulate matter. *Nature* 332., 341-343.
- BLEAHU, M. (1976): Structural position of the Apuseni Mountains in the Alpine system. *Rev. Roum. Géol. Géophys. Géogr., Ser. Géol.* 20., 7-19.
- BORBÉLY-KISS, I., KOLTAY, E., LÁSZLÓ, S., SZABÓ, GY., ZOLNAI, L. (1985): Experimental and Theoretical Calibration of a PIXE Setup for K and L-Rays. *Nucl. Instr. and Meth. in Phys. Res. B12.*, 496-504.
- BOTTJER, D. J., ARTHUR, M. A., DEAN, W. E., HATTIN, D. E., SAVRDA, C. E. (1986): Rhythmic bedding produced in Cretaceous pelagic carbonate environments: sensitive recorders of climatic cycles. *Paleoceanography* 1., 467-481.
- BRULAND, K. W. (1983): Trace elements in seawater. In: RILEY, J. P., CHESTER, R. (eds.): *Chemical Oceanography*, 157-220. Academic Press, New York.
- CORNIDES, I., CSÁSZÁR, G., HAAS, J., JOCHA-EDELÉNYI, E. (1979): Oxigén izotópos hőmérséklet-mérések a Dunántúl mezozoós képződményeiből. (In Hungarian with English abstract. Temperature measurements of Transdanubian Mesozoic rocks by the oxygen isotope method) *Földt. Közl.* 109., 101-110.
- DEAN, W. E., GARDNER, J. V., PIPER, D. Z. (1997): Inorganic geochemical indicators of glacial-interglacial changes in productivity and anoxia on the California continental margin. *Geochim. Cosmochim. Acta* 61/21., 4507-4518.



- DE BOER, P. L., SMITH, D. G. (1994): Orbital forcing and cyclic sequences. In: DE BOER, P. L. and SMITH, D. G. (Eds): *Orbital Forcing and Cyclic Sequences*. IAS Spec. Publ. 19., 1-14.
- DICKENS, G. R., OWEN, R. M. (1994): Late Miocene-Early Pliocene manganese redirection in the central Indian Ocean. Expansion of the intermediate water oxygen minimum zone. *Paleoceanography* 9., 161-181.
- EINSELE, G., RICKEN, W., SEILACHER, A. (1991): Cycles and events in stratigraphy - basic concepts and terms. In: EINSELE, G., RICKEN, W., SEILACHER, A. (Eds): *Cycles and Events in Stratigraphy*. Springer, Berlin, 1-9.
- ERBA, E., PREMOLI SILVA, I. (1994): Orbitally driven cycles in trace fossils distribution from the Piobbico core (late Albian, central Italy). In: DE BOER, P. L. and SMITH, D. G. (Eds): *Orbital Forcing and Cyclic Sequences*. IAS Spec. Publ. 19., 211-225.
- FISCHER, A. G., DE BOER, P. L., PREMOLI SILVA, I. (1990): Cyclostratigraphy. In: GINSBURG, R. N. and BEAUDOIN, B. (Eds): *Cretaceous Resources, Events and Rhythms - Background and Plans for Research*. Kluwer, Dordrecht, 139-172.
- FISHER, N. S., GUILLARD, R. R. L., BANKSTON, D. C. (1991): The accumulation of barium in marine phytoplankton grown in culture. *J. Mar. Res.* 49., 339-354.
- FOGARASI, A. (1995): Ciklussztratigráfiai vizsgálatok a gerecsei krétában: előzetes eredmények. (In Hungarian with English abstract. Cretaceous cyclostratigraphy of Gerecse Mts. Preliminary results.) *Ált. Földt. Szemle* 27., 43-58.
- FORCE, E. R., CANNON, W. F. (1988): Depositional model for shallow-marine manganese deposits around black shale basins. *Econ. Geol.* 83., 93-117.
- FROELICH, P. N., BENDER, M. L., LUEDTKE, N. A., HEATH, G. R., DEVRIES, T. (1982): The marine phosphorous cycle. *Amer. J. Sci.* 282., 474-511.
- FÜLÖP, J., BREZSNYÁNSZKY, K., HAAS, J. (1987): The new map of basin basement of Hungary. *Acta Geol. Hung.* 30., 1-2, 3-20.
- GOBEIL, C., MACDONALD, R. W., SUNDBY, B. (1997): Diagenetic separation of cadmium and manganese in suboxic continental margin sediments. *Geochim. Cosmochim. Acta* 61/21., 4647-4654.
- GOLDBERG, E. D., ARRHENIUS, G. O. S. (1958): Chemistry of Pacific pelagic sediments. *Geochim. Cosmochim. Acta* 13., 153-212.
- GROW, J. A., MATTICK, R. E., BÉRCZY-MAKK, A., PÉRÓ, CS., HAJDÚ, D., POGÁCSÁS, GY., VÁRNAI, P., VARGA, E. (1994): Structure of the Békés Basin Inferred from Seismic Reflection, Well and Gravity Data. In: TELEKI, P. G. et al. (Eds.): *Basin Analysis in Petroleum Exploration*. Kluwer, Dordrecht, 1-38
- HAAS, J. (1994): Magyarország geológiája – Mezozoikum. Egyetemi jegyzet. (Geology of Hungary - Mesozoic. Lecture notes.) Eötvös Loránd Tudományegyetem, Budapest. (University of Loránd Eötvös, Budapest) 199 p. (In Hungarian)
- HALLAM, A. (1964): Origin of the limestone-shale rhythm in the Blue Lias of England: a composite theory. *Jour. Geol.* 72. 157-169.
- HATCH, J. R., LEVENTHAL, J. S. (1992): Relationship between inferred redox potential of the depositional environment and geochemistry of the Upper Pennsylvanian (Missourian) Stark Shale Member of the Dennis Limestone, Wabunsee County, Kansas, U.S.A.. *Chem. Geol.* 99., 65-82.
- HUERTA-DIAZ, M. A., MORSE, J. W. (1992): Pyritization of trace metals in anoxic marine sediments. *Geochim. Cosmochim. Acta* 56., 2681-2702.
- IANOVICI, V., BORCOS, M., BLEAHU, M., PATRULIUS, D., LUPU, M., DIMITRESCU, R., SAVU, H. (1976): *Geologia Muntilor Apuseni*. (Geology of Apuseni Mountains) Edit. Acad. R. S. R. 631 p. Bucuresti.
- JENKYN, H. C., GALE, A. S., CORFIELD, R. M. (1994): Carbon- and oxygen-isotope stratigraphy of the English Chalk and Italian Scaglia and its paleoclimatic significance. *Geol. Mag.* 131., 1-34.
- JOHANSSON, S.A.E., CAMPBELL, J.L. (Eds.) (1988): *PIXE: A Novel Technique for Elemental Analysis*, John Wiley & Sons, Chichester.
- KUMAR, N., ANDERSON, R. F., BISCAYE, P. E. (1996): Remineralization of particulate authigenic trace metals in the Middle Atlantic Bight: Implications for proxies of export production. *Geochim. Cosmochim. Acta* 60., 3383-3397.
- LEWAN, M. D., MAYNARD, J. B. (1982): Factors controlling enrichment of vanadium and nickel in the bitumen of organic sedimentary rocks. *Geochim. Cosmochim. Acta* 46., 2547-2560.
- MACHHOUR, L., PHILIP, J., OUDIN, J. L. (1994): Formation of laminite deposits in anaerobic-dysaerobic marine environments. *Mar. Geol.* 117., 287-302.
- MATTIOLI, E. (1997): Nannoplankton productivity and diagenesis in the rhythmically bedded Toarcian-Aalenian Fiuminata section (Umbria-Marche Apennine, central Italy). *Palaeogeog., Palaeoclim., Palaeoecol.* 130., 113-133.

- MURRAY, R. W., LEINEN, M. (1993): Chemical transport to the seafloor of the equatorial Pacific Ocean across a latitudinal transect at 135° W: Tracking sedimentary major, trace and rare earth element fluxes at the Equator and the Intertropical Convergence Zone. *Geochim. Cosmochim. Acta* 57., 4141-4163.
- MURRAY, R. W., LEINEN, M. (1996): Scavenged excess aluminium and its relationship to bulk titanium in biogenic sediment from the central equatorial Pacific Ocean. *Geochim. Cosmochim. Acta* 60., 3869-3878.
- MURRAY, R. W., BUCHHOLTZ TEN BRINK, M. R., JONES, D. L., GERLACH, D. C., RUSS G. P. III. (1990): Rare earth elements as indicators of different marine depositional environments in chert and shale. *Geology* 18., 268-271.
- MURRAY, R. W., BUCHHOLTZ TEN BRINK, M. R., GERLACH, D. C., RUSS G. P. III., JONES, D. L. (1991): Rare earth, major, and trace elements in chert from the Franciscan Complex and Monterey Group, California, assessing REE sources to fine grained marine sediments. *Geochim. Cosmochim. Acta* 55., 1875-1896.
- MURRAY, R. W., LEINEN, M., ISEM, A. R. (1993): Biogenic flux of Al to sediment in the central equatorial Pacific Ocean. Evidence for increased productivity during glacial periods. *Paleoceanography* 8., 651-670.
- NAGY, E. (1969): A Mecsek hegység alsóliász kőszénösszlete. *Földtan. (Lower Liassic coal formation of the Mecsek Mountains. Geology.) MAFI Évkönyve (Annals of Hung. Inst. of Geol.)* 51/2., 245-971. (In Hungarian).
- NATH, B. N., ROELANDTS, I., SUDHAKAR, M., PLUEGER, W. L. (1992): Rare earth element patterns of the Central Indian Basin sediments related to their lithology. *Geophys. Res. Letts.* 19., 1197-1200.
- ODERMATT, J. R., CURIALE, J. A. (1991): Organically bound metals and biomarkers in the Monterey Formation of the Santa Maria Basin, California. *Chem. Geol.* 91., 99-113.
- PINGITORE, N. E. JR., LYTLE, F. W., DAVIES, B. M., EASTMAN, M. P., ELLER, P. G., LARSON, E. M. (1992): Mode of incorporation of Sr in calcite: determination by X-ray absorption spectroscopy. *Geochim. Cosmochim. Acta* 56., 1531-1538.
- PIPER, D. J. W., STOW, D. A. V. (1991): Fine-grained turbidites. In: EINSELE, G., RICKEN, W., SEILACHER, A. (Eds): *Cycles and Events in Stratigraphy*. Springer, Berlin, 360-376.
- PRANGE, A., KREMLING, K. (1985): Distribution of dissolved molybdenum, uranium and vanadium in Baltic Sea waters. *Mar. Chem.* 16., 259-274.
- RAUCSIK, B. (1997): Stable isotopic composition of the Komló Calcareous Marl Formation („Spotted marl” s. str.), Mecsek Mountains, S Hungary. *Acta Min.-Petr., Szeged* 38., 95-109.
- RICKEN, W. (1991): Variation of sedimentation rates in rhythmically bedded sediments. Distinction between depositional types. In: EINSELE, G., RICKEN, W., SEILACHER, A. (Eds): *Cycles and Events in Stratigraphy*. Springer, Berlin, 167-187.
- RICKEN, W. (1994): Complex rhythmic sedimentation related to third order sea-level variations: Upper Cretaceous, Western Interior Basin, USA. In: DE BOER, P. L. and SMITH, D. G. (Eds): *Orbital Forcing and Cyclic Sequences*. IAS Spec. Publ. 19., 167-193.
- ROCC Group (Research on Cretaceous Cycles Group) (1986): Rhythmic bedding in Upper Cretaceous pelagic carbonate sequences: varying sedimentary response to climatic forcing. *Geology* 14., 153-156.
- SAAGER, P. M., DE BAAR, H. J. W., BURKILL, P. H. (1989): Manganese and iron in Indian Ocean waters. *Geochim. Cosmochim. Acta* 53., 2259-2267.
- SAVRDA, C. E., BOTTJER, D. J. (1994): Ichnofossils and ichnofabrics in rhythmically bedded pelagic/hemipelagic carbonates: recognition and evaluation of benthic redox and scour cycles. In: DE BOER, P. L. and SMITH, D. G. (Eds): *Orbital Forcing and Cyclic Sequences*. IAS Spec. Publ. 19., 195-210.
- SAVRDA, C. E., BOTTJER, D. J., SEILACHER, A. (1991): Redox-related benthic events. In: EINSELE, G., RICKEN, W., SEILACHER, A. (Eds): *Cycles and Events in Stratigraphy*. Springer, Berlin, 524-541.
- SCHROEDER, J. O., MURRAY, R. W., LEINEN, M., PFLAUM, R. C., JANECEK, T. R. (1997): Barium in equatorial Pacific carbonate sediment: Terrigenous, oxide, and biogenic associations. *Paleoceanography* 12., 125-146.
- SETHI, P. S., LEITHOLD, E. L. (1994): Climatic cyclicality and terrigenous sediment influx to the Early Turonian Greenhorn Sea, southern Utah. *J. of Sed. Research B* 64/1., 26-39.
- SHAW, T. J., GIESKES, J. M., JAHNKE, R. A. (1990): Early diagenesis in differing depositional environments: The response of transition metals in pore water. *Geochim. Cosmochim. Acta* 54., 1233-1246.
- SUNDARAMAN, P., SCHOELL, M., LITKE, R., BAKER, D. R., LEYTHAEUSER, D., RULLKÖTTER, J. (1993): Depositional environment of Toarcian shales from northern Germany as monitored with porphyrins. *Geochim. Cosmochim. Acta* 57., 4213-4218.
- SZABÓ, GY., BORBÉLY-KISS, I. (1993): PIXYKLM Computer Package for PIXE Analyses. *Nucl. Instr. and Meth. in Phys. Res. B* 75., 123-126.
- TAYLOR, S. R., MCLENNAN, S. M. (1985): *The Continental Crust, Its Composition and Evolution*. Blackwell Scientific Publications, Oxford, London.

- TUCKER, M. E., WRIGHT, V. P. (1990): Carbonate sedimentology. Blackwell Scientific Publications, Oxford, London.
- TUREKIAN, K. K. (1972): Chemistry of the Earth. Holt, Rinehart, and Winston.
- WEDEPOHL, K. H. (1978): Manganese: abundance in common sediments and sedimentary rocks. In: Handbook of Geochemistry. Springer, Berlin, II/3., 1-17.
- WEISSERT, H., BRÉHÉRET, J. G. (1991): A carbonate carbon-isotope record from the Aptian-Albian sediments of the Vocontian trough (SE France). Bull. Soc. Géol. Fr. 162., 1133-1140.

*Manuscript received 16 October, 1998.*

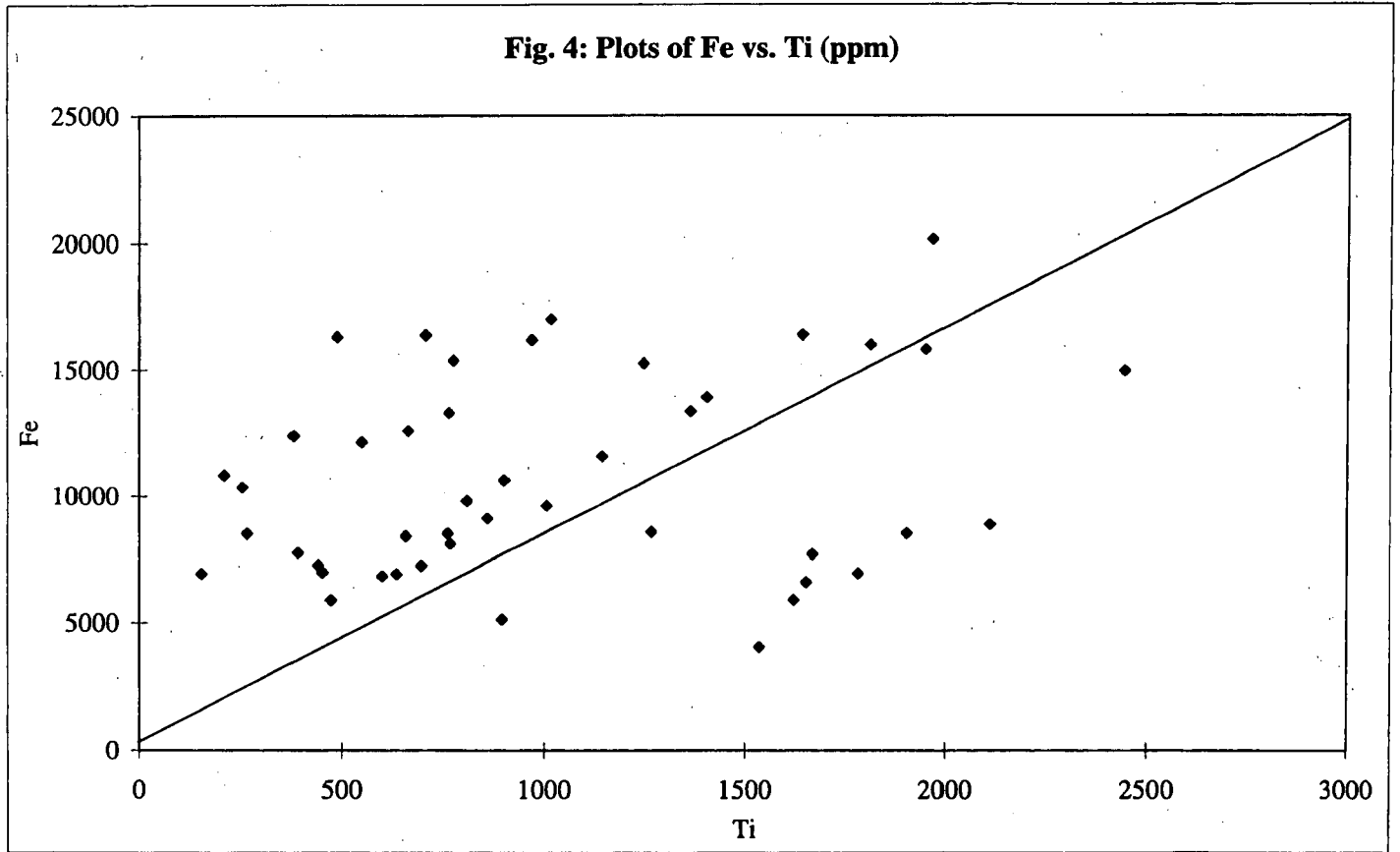




Fig. 5: Fe/Ti ratios of the measured samples

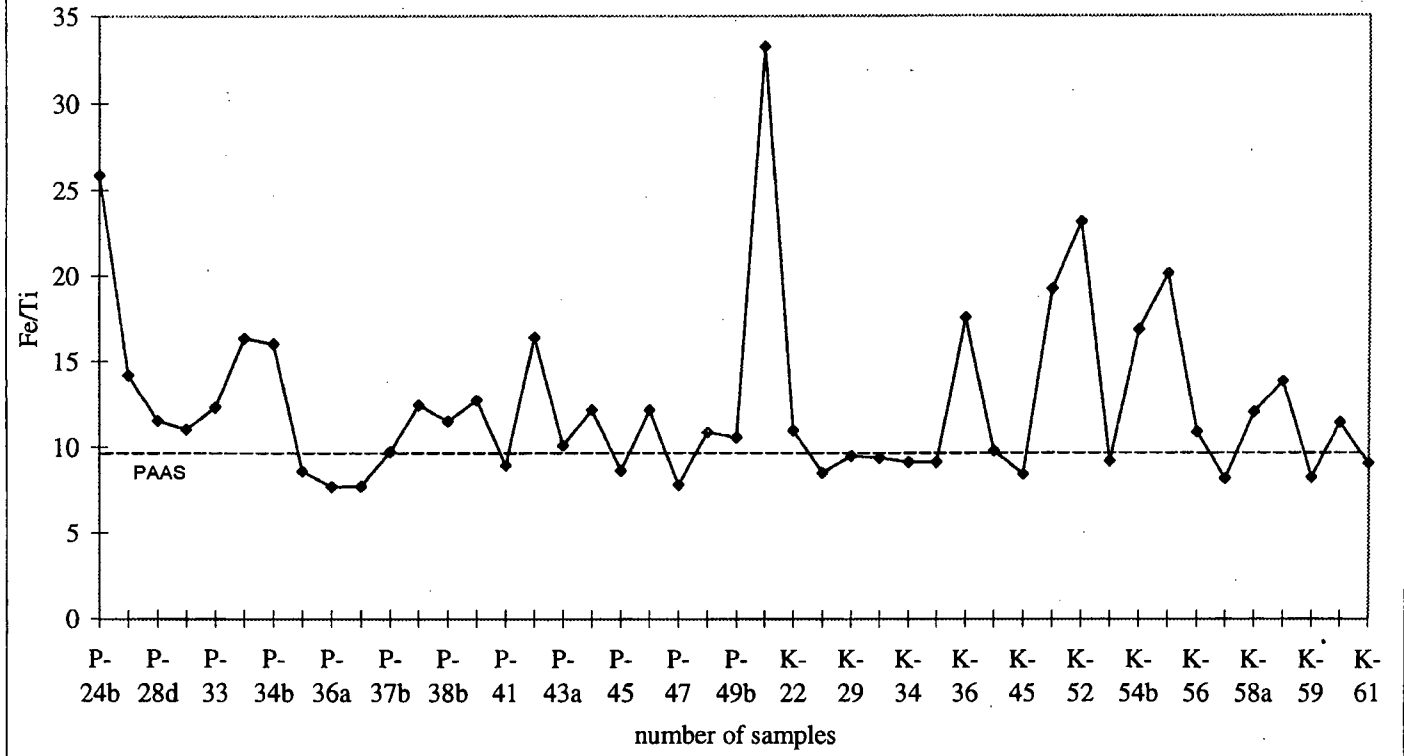
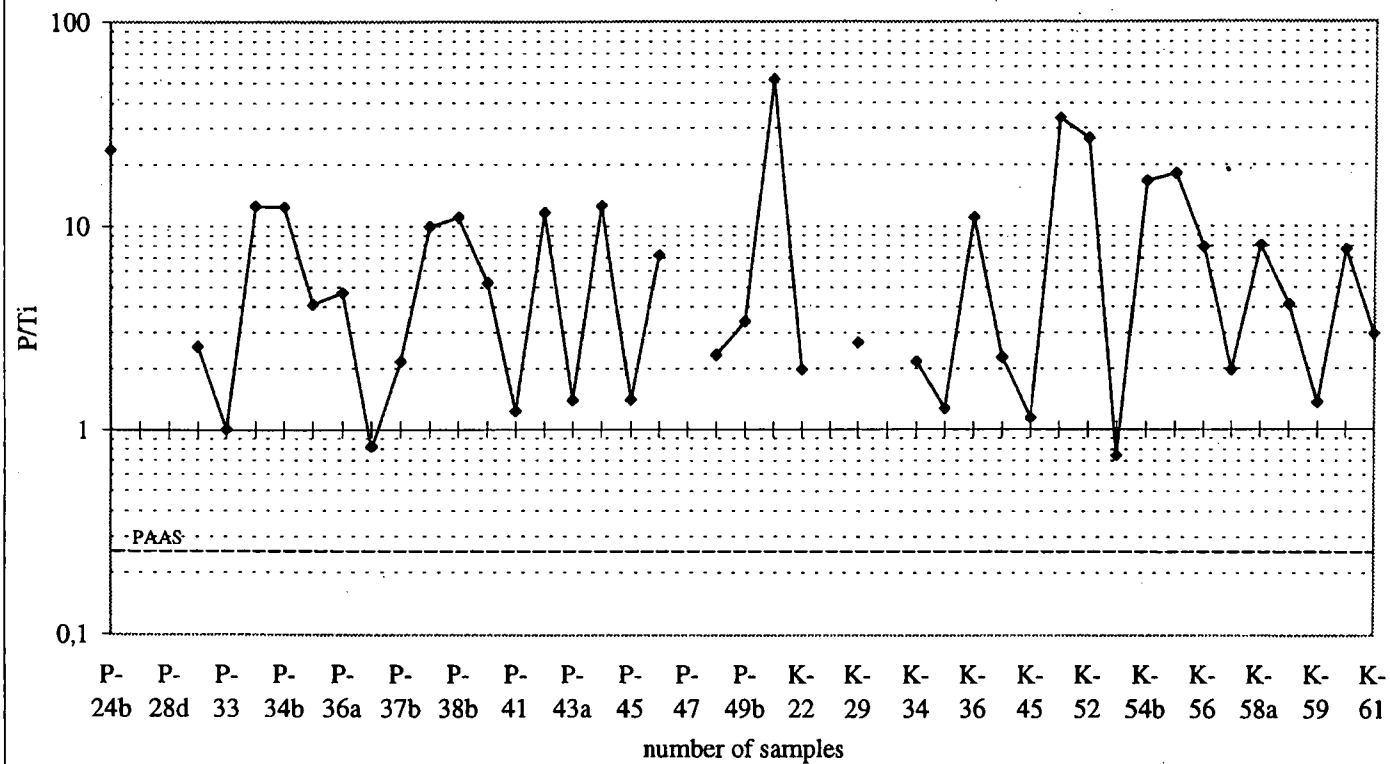
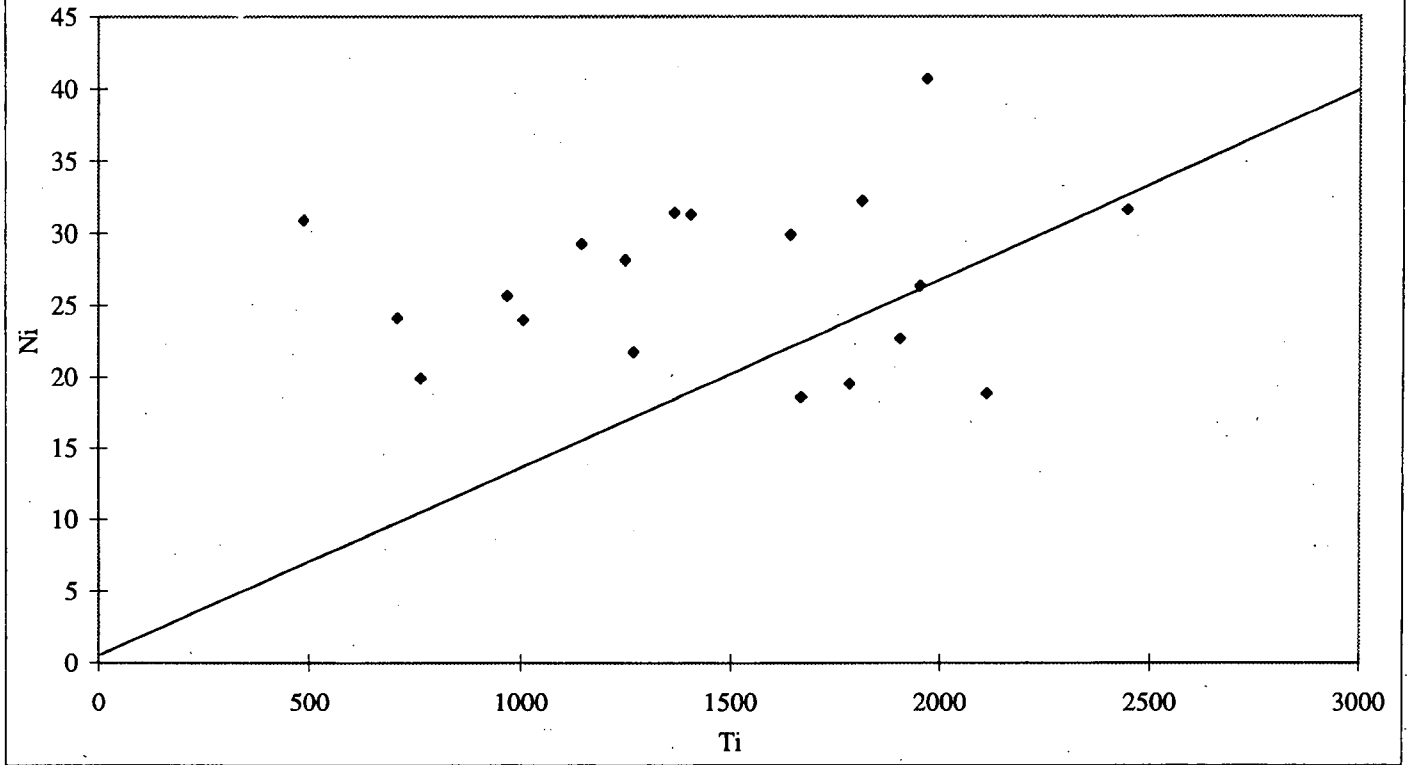


Fig. 6: P/Ti ratios of the measured samples



**Fig. 7: Plots of Ni vs. Ti (ppm)**



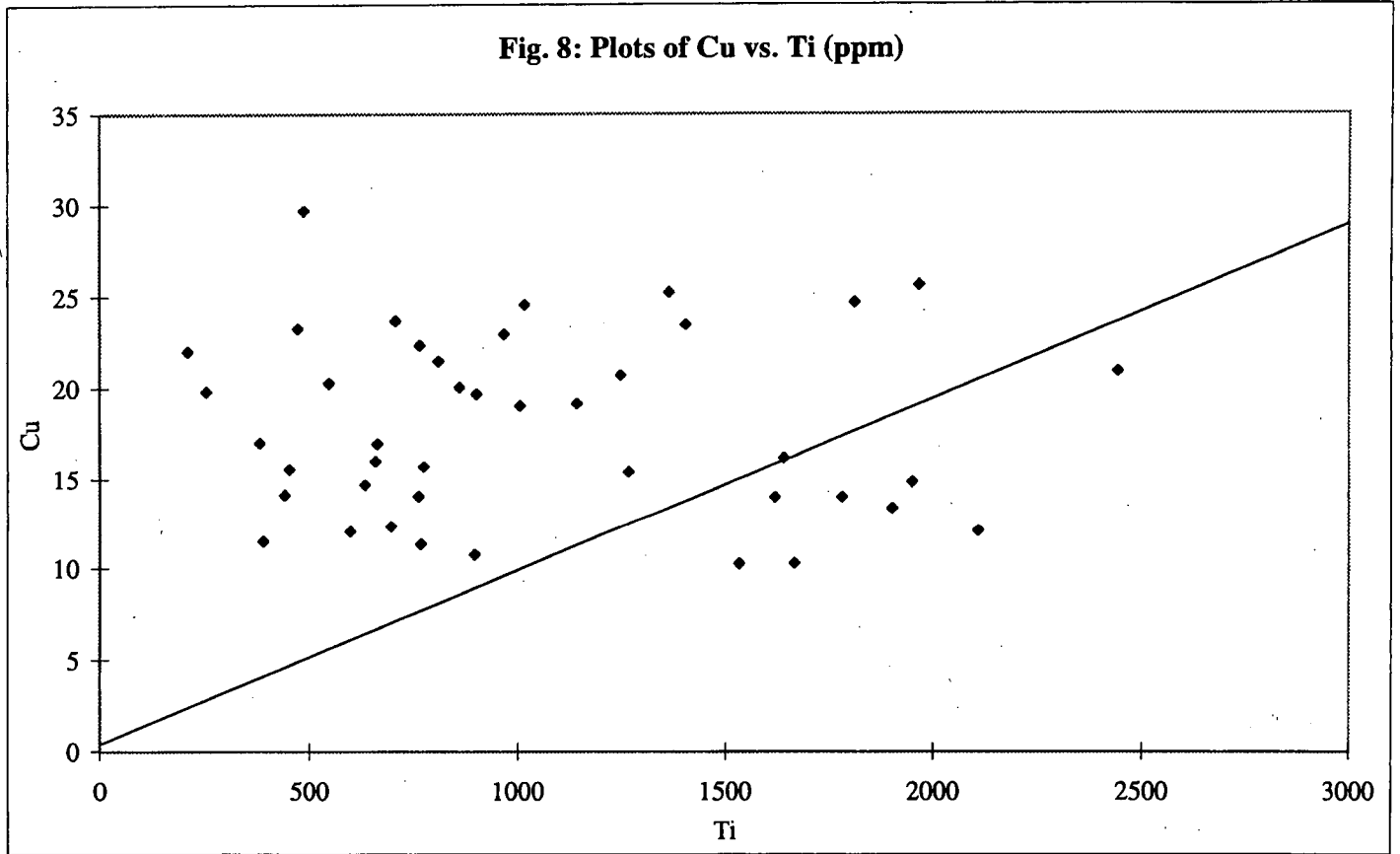
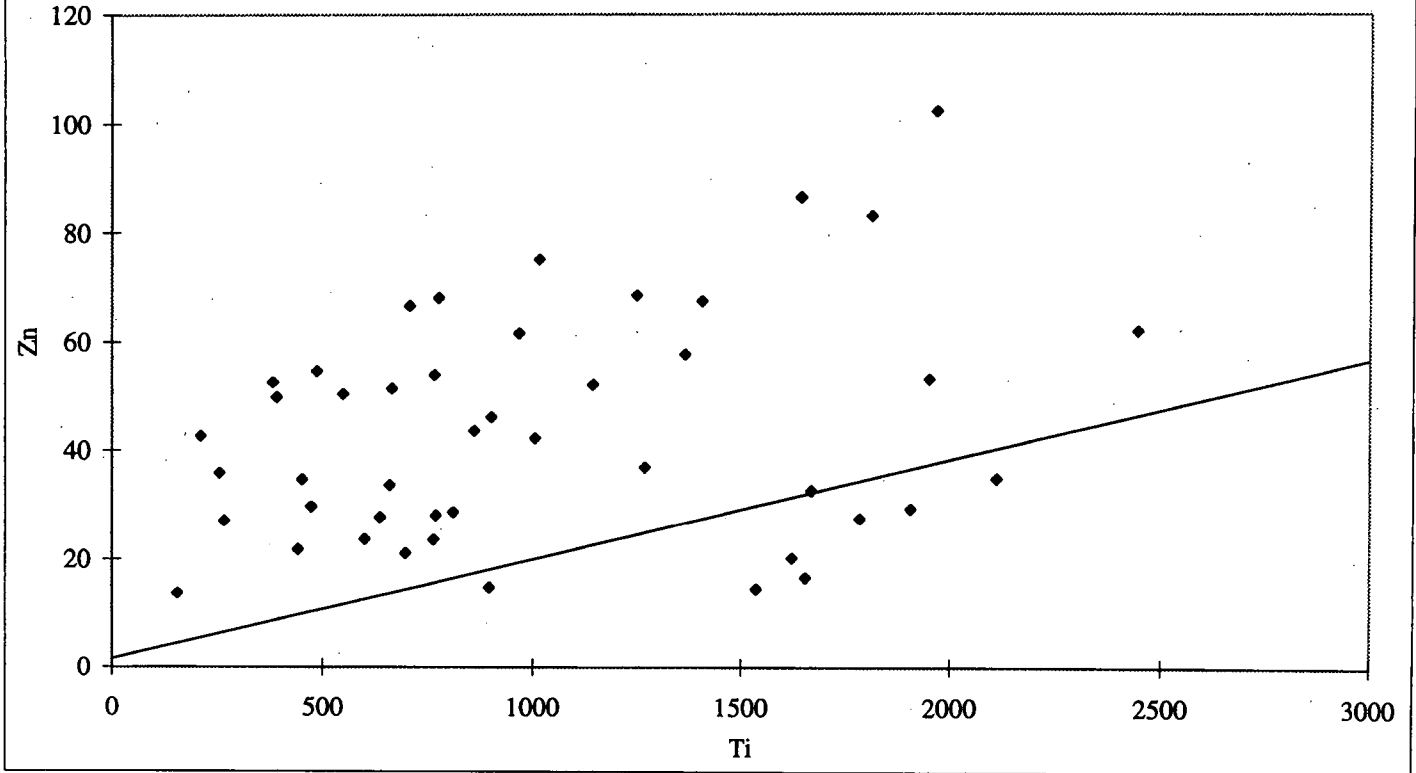


Fig. 9: Plots of Zn vs. Ti (ppm)



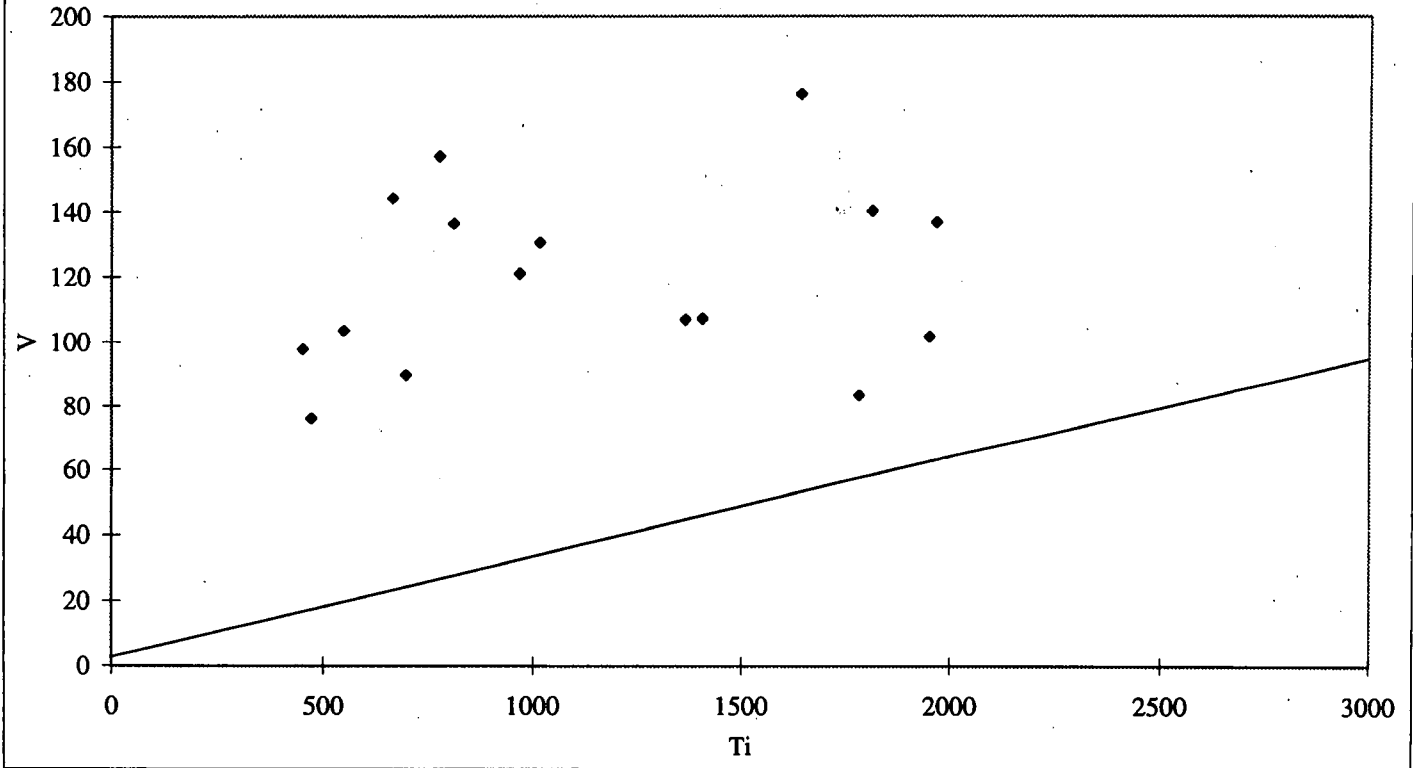
**Fig. 10: Plots of V vs. Ti (ppm)**

Fig. 11: Plots of Sr vs. Ti (ppm)

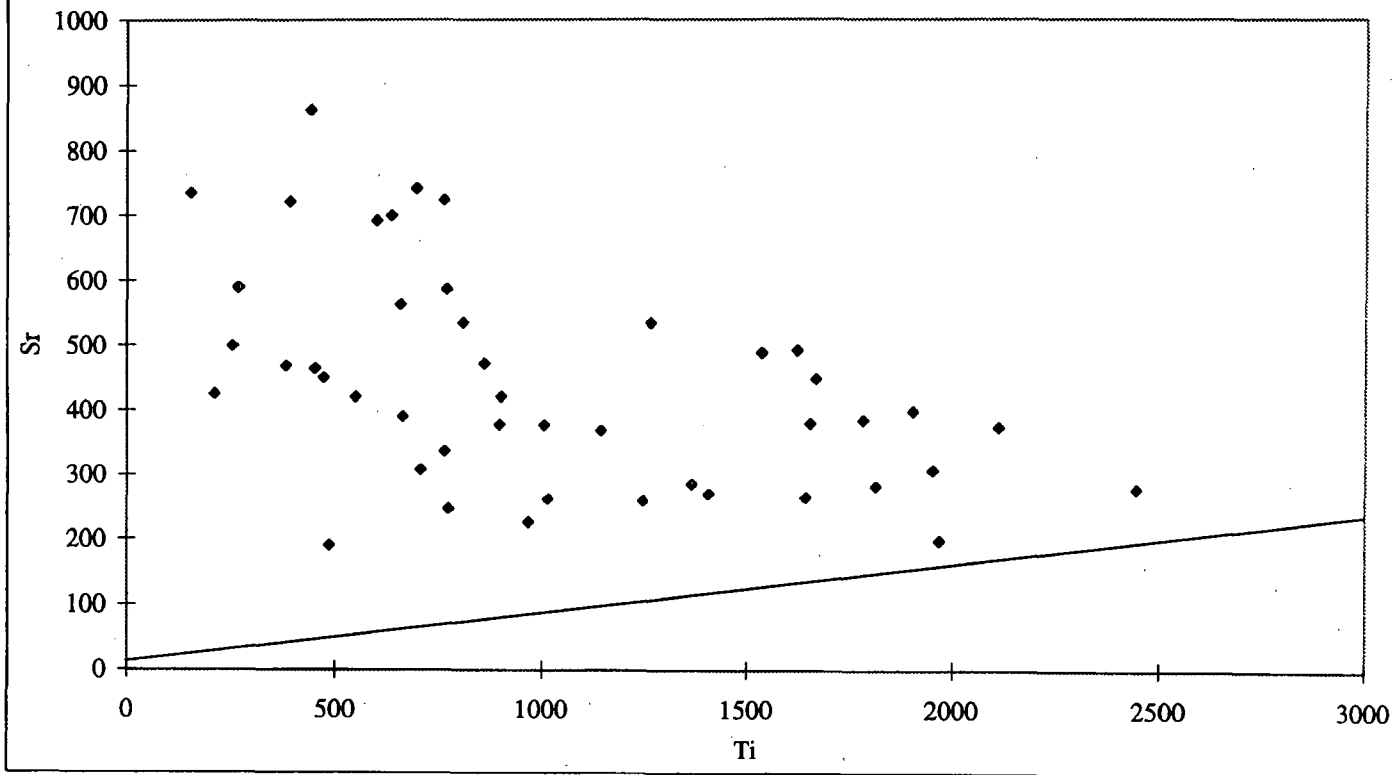


Fig. 12: Cu and Zn values of the measured samples

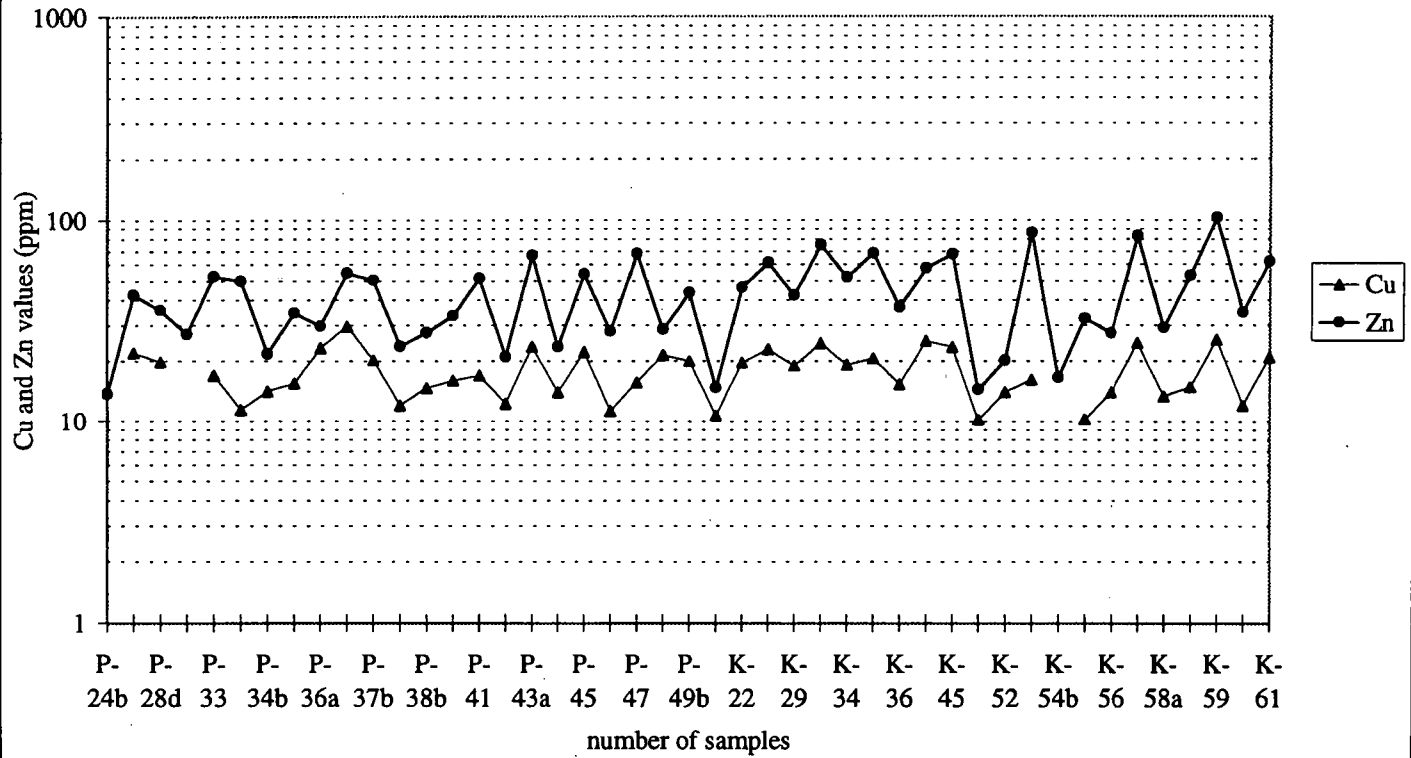




Fig. 13: Sr/Ti ratios of the measured samples

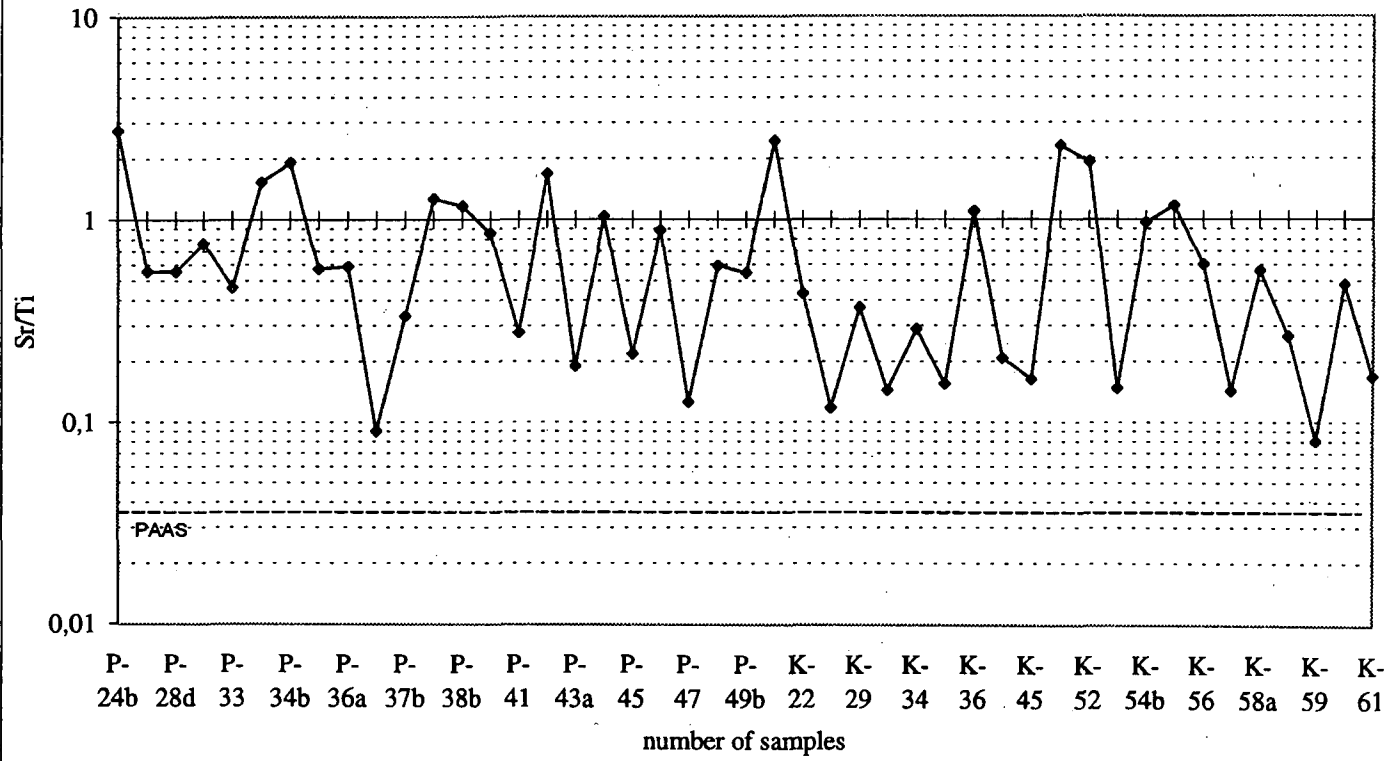
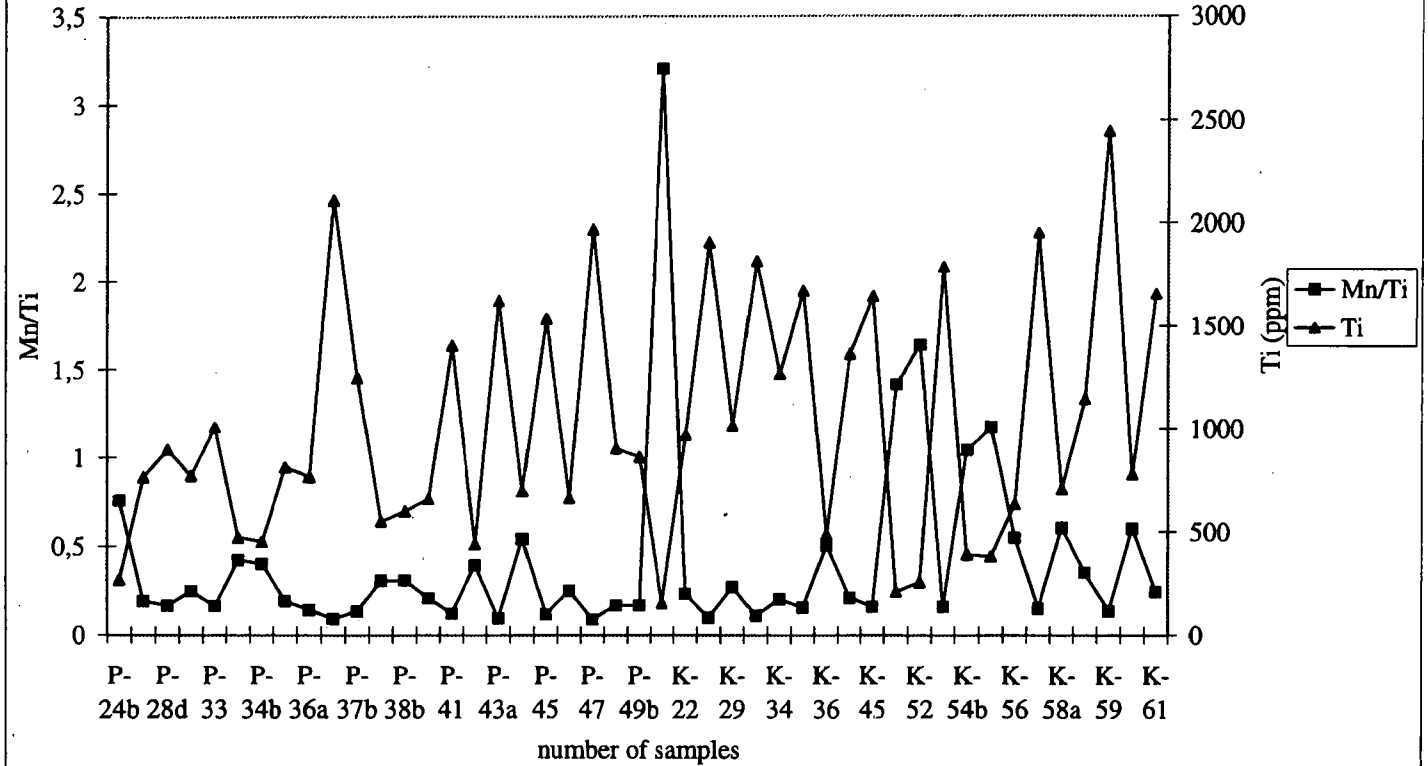
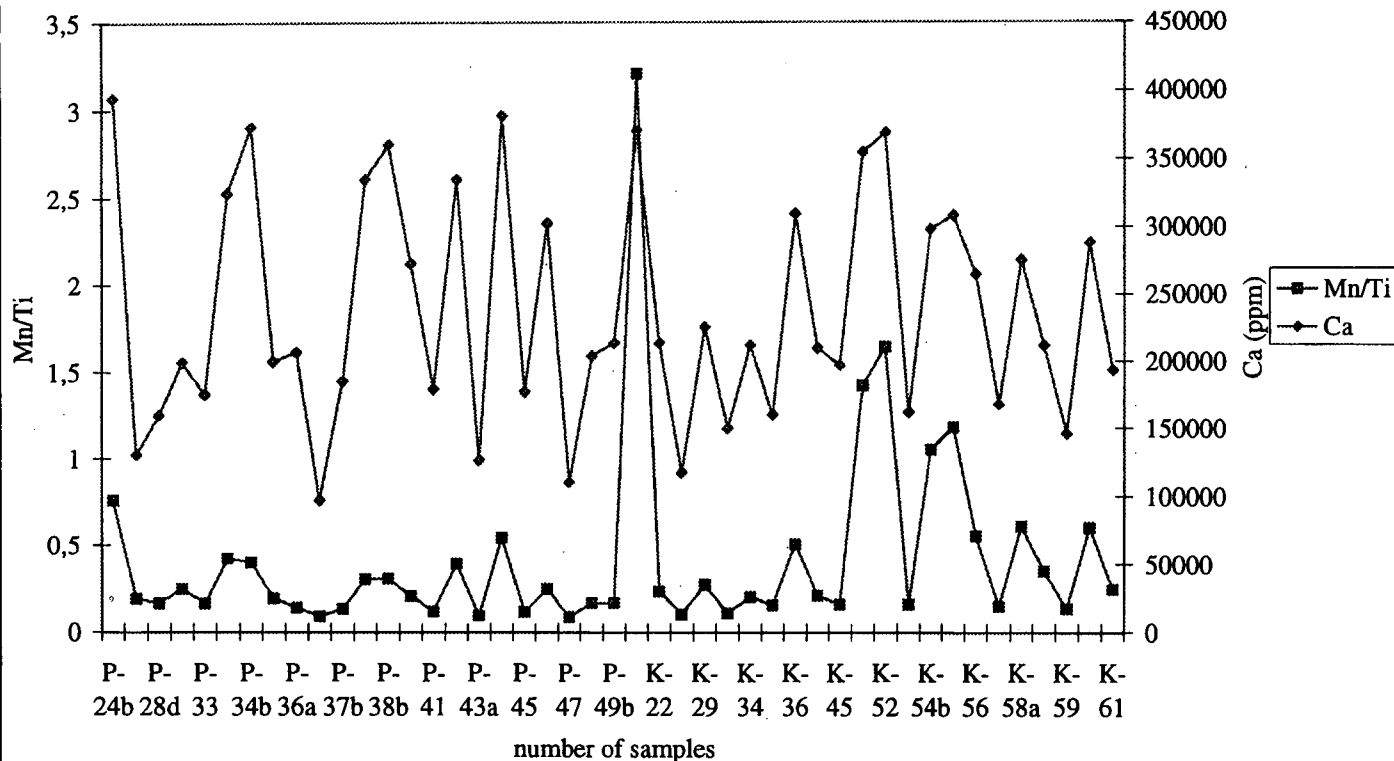


Fig. 14a: Mn/Ti ratios and Ti values of the measured samples



**Fig. 14b: Mn/Ti ratios and Ca values of the measured samples**



**Fig. 15: Fe/Mn ratios of the measured samples**

